LONG TIME STRESS RELAXATION OF UNFILLED AND FILLED AMORPHOUS NETWORKS UNDER UNIAXIAL TENSION

by

HALUK KONYALI

Submitted to the Graduate School of Engineering and Natural Sciences
in partial fulfillment of
the requirements for the degree of
Doctor of Philosophy

Sabanci University

June 2008

LONG TIME STRESS RELAXATION OF UNFILLED AND FILLED AMORPHOUS NETWORKS UNDER UNIAXIAL TENSION

APPROVED BY:

Prof. Dr. Yusuf Z. Menceloğlu (Thesis Supervisor)	……
Prof. Dr. Burak Erman (Thesis Co-advisor)	……
Prof. Dr. Atilla Güngör	…….
Asst. Prof. Melih Papila	……
Asst. Prof. Mehmet Yıldız	……

DATE OF APPROVAL: ……

LONG TIME STRESS RELAXATION OF UNFILLED AND FILLED AMORPHOUS NETWORKS UNDER UNIAXIAL TENSION

Haluk KONYALI

MAT, PhD Thesis, 2008

Thesis Supervisor: Prof. Dr. Yusuf Z. MENCELOĞLU

Thesis Co-advisor Prof. Dr. Burak ERMAN

Keywords: Dynamic Constrained Junction Model, relaxation, amorphous networks

ABSTRACT

The stress relaxation of amorphous filled and unfilled networks is the main objective of the present study. For this purpose, unfilled and filled samples having different cross-link densities and filler loadings were prepared. Stress relaxation tests were performed on a universal tensile test equipment. Constrained Junction Model, which is the model for the amorphous networks at equilibrium, was extended for the stress relaxation of the amorphous networks. For the unfilled section, it was assumed that the parameter which is the measure of the strength of the constraints in Constrained Junction Model follows the stretched exponential form. Experimental results showed that the new theory called Dynamic Constrained Junction Model can very well capture the isochronous Mooney plots and the relaxation of the stress for the unfilled samples. For the filled samples, the new theory was further extended with the second assumption that the phantom, equilibrium and non-equilibrium forces in the Dynamic Constrained Junction Model follow the Guth and Gold viscosity relation when fillers are added into the matrix. The experimental results showed that the Dynamic Constrained Junction Model can well capture the isochronous Mooney plots and stress relaxation of the networks in filled state.

TEK YÖNLÜ ÇEKMEDE DOLGULU VE DOLGUSUZ AMORF AĞLARIN UZUN SÜRELİ GERİLME GEVŞEMESİ

Haluk KONYALI

MAT, Doktora Tezi, 2008

Tez Danışmanı: Prof. Dr.Yusuf Z. MENCELOĞLU

Tez Yardımcı Danışmanı: Prof. Dr. Burak ERMAN

Anahtar Kelimeler: Dinamik Kaucuk Elastisitesi Modeli (Dynamic Constrained Junction Model), gevşeme, amorf ağlar

ÖZET

Bu çalışmanın amacı dolgulu ve dolgusuz ağların gerilme gevşemesidir. Bu amaçla, farklı dolgu oranlı ve çapraz bağlı numuneler hazırlandı. Gerilme gevşeme deneyleri evrensel çekme makinasında yapıldı. Denge halindeki amorf ağların modeli için kullanılan kaucuk elastisite modeli (Constrained Junction Model), amorf ağların gerilme gevşemesi için genişletildi. Dolgusuz kısım için, kauçuk elastisitesi modelinde düğüm noktalarına gelen kuvvetinin bir ölçüsü olan parametrenin çekilmiş exponansiyel forma uyduğu varsayımı yapılmıştır. Deneysel sonuçlar göstermiştir ki, dinamik kauçuk elastisitesi diye adlandırılan bu yeni model ile dolgusuz numunelerin Mooney eşzaman eğrileri ve gerilme gevşemeleri çok iyi yakalanmıştır. Dolgulu numuneler için, dolgu matrise eklendiğinde, denge ve denge dışı kuvvetlerin Guth ve Gold vizkosite ilişkisine uyduğu ikinci varsayımı yapılmıştır. Deneysel sonuçlar göstermiştir ki, dinamik kauçuk elastisitesi modeli dolgulu numunelerde Mooney eşzaman eğrilerini ve gerilme gevşemesini iyi derecede yakalamıştır.

Sevgili eşim Tolunay ve sevgili oğlum Deniz'e…

ACKNOWLEDGEMENTS

I would like to express my deepest appreciation to Prof. Dr. Burak Erman and Prof. Dr. Yusuf Menceloğlu for their encouraging guidance, advice, helpful criticism and invaluable supervision throughout the course of this study.

I am also grateful to my thesis committee members Prof. Dr. Atilla Güngör, Asst. Prof. Melih Papila and Asst. Prof. Mehmet Yıldız for their valuable review and comments on the dissertation.

I would like to extend my special thanks to Dr. Yavuz Dogan, not only for giving this opportunity to me but also supporting and trusting me all the way long. I felt confident and strong with his encourgement throughout this study.

Special thanks to Dr. Funda İnceoğlu for her patients and help especially during the qualification exam and the preparation of this thesis. I am also thankful to Dr. Kazım Acatay and Dr. İlhan Özen for their friendship.

I am also particularly grateful to my wife Tolunay Konyalı for her endless love and encouragement. Her understanding is beyond all appreciation during my education. I love my son, Deniz Konyalı and special thanks to him for relaxing me with his endless energy when I am under pressure.

I would like to express my deepest thanks and appreciation to my family for their understanding, motivation, encouregement, and their respect to my academic life. I feel their love and pray throughout all my education life.

TABLE OF CONTENTS

LIST OF FIGURES

LIST OF TABLES

LIST OF NOMENCLATURES

N_A	Avagadro's number
k	Boltzmann constant
F	Elastic force
E	Energy
r	End to end vector
S	Entropy
H	Enthalpy
G	Gibbs free energy
A	Helmholtz free energy
Q	Heat
L	Length
$2C_1$,$2C_2$	Material constants in Mooney Rivlin
P	Probability density function
P	Pressure
f^*	Reduced stress
W	Work
Z	Strain energy function
I	Strain invariant
y	Strain tensor
T	Temperature
M_e	The average molecular weight between junctions
M	Weight
V	Volume
ξ	Cycle rank
ρ	Density

ϕ	Effective volume fraction
θ	Functionality of a junction
κ	Strength of constraints
λ	Stretch ratio
ν	The number of network chains
μ	The number of junctions

LIST OF ABBREVIATIONS

FEF	Fast extrusion furnace (carbon black)
HAF	High abrasion furnace (carbon black)
NR	Natural Rubber
BR	Polybutadiene Rubber
SBR	Styrene Butadiene Rubber

CHAPTER 1

1. INTRODUCTION

In this section, the basic information about polymers and especially elastomers will be discussed. The molecular background and the basic postulates of the rubberlike elasticity will be given. Since this study is based on the one of the most famous viscoelastic theory called Constrained Junction Model, this model and the other basic molecular origin based viscoelastic theories will be given in detail. The Mooney Rivlin equation which is the phenomenological based viscoelastic theory will be discussed at the end.

1.1 Rubbery Materials

Polymeric materials have been divided into main two groups, thermoplastics and thermosets, in terms of their behavior at elevated temperatures or, alternately upon whether the polymeric material is cross-linked or not, which is the key structural feature that determines behavior at high temperatures. For the sake of convenience of classification, polymers are named as elastomers if they have more than two hundred per cent elastic elongation. Elastic elongation is defined as the one that any material experience below their yield point, widely referred as the elastic limit. The elongation beyond the yield point is called inelastic meaning that the elongation will cause a permanent deformation; hence full recovery to the original length is not possible. Therefore, elongation beyond the yield point is inelastomeric.

Elastomers can be repeatedly stretched over at least twice to their normal length and return to their original length on the removal of force. Elastomers may be either

thermoplastics or thermosets. If they are thermosets, they are so lightly cross-linked that hardening does not occur. It is due to the cross-linking that they cannot be melted after curing.

All materials have some elastic elongation, but for most of the materials, especially metals, the elastic region is very small. For metals the elastic elongation is less than two per cent. Some plastic materials which are referred to as engineering plastics have elastic elongations in the same range as metals; whereas others, for example well known plastic such as, polyethylene, can have elastic elongations up to fifty per cent. [1].

High strength and high stiffness in materials are related to the crystalline structures, other strong interactions between the molecules or atoms, and general stiffness of the molecules. Easy movement of the molecules relative to each other is prevented due to these features and decrease elastic elongation. The elastomers, therefore, have opposite structural features. Elastomeric materials are highly random, in general totally amorphous, and have few strong interactions between chains. Flexible polymer chains are of usually aliphatic nature rather than aromatic nature. The molecules can easily move relative to each other if a tensile force is applied on to an elastomer, probably just a simple uncoiling of the tangled molecules. This movement goes on like that with little additional force until the molecules are totally stretched or some other means of resistance is overcome.

Up on the removal of tensile force, the molecules will turn back to their original, random shape and the whole structure will return to its original shape. The recover of this elastic region will occur provided that the molecules have not been displaced in absolute position to one another. In other words, they have not slid but have uncoiled. If sliding happens, the elastic limit (yield point) will be exceeded and some inelastic movement will be introduced. This inelastic movement cannot be recovered [1].

The tendency of the elastomeric material to return to its original, random state on the removal of force is attributed to entropy. Entropy is a measure of disorder of a system. Because of the high randomness, the non-stressed state has the highest entropy. When the external tensile force is applied to the system, order of the molecules will increase and entropy is forced to decrease. From thermodynamics' point of view this is a less favorable or

unstable state. Therefore, on the removal of external force, the entropy will naturally try to increase. This is the driving force for the system to return to the original, random state [2].

When the chains are forced into more ordered positions by stretching the elastomer and reducing entropy, the total energy of the system will be lower, heat will be released and a slight warming of the sample will be detected. After relaxation of the applied force, heat goes into the material to be able to have the randomness and a cooling is realized because the heat is being taken in.

Since the elastomers are different from the other materials in terms of the entropy based elasticity, here some basic thermodynamic equations will be given for elastomers.

The change in internal energy E accompanying the stretching of an elastic body may be written with complete generality as follows [3]:

$$dE = \delta Q - \delta W \tag{1.1}$$

Where, the differential heat absorbed by is δQ and the differential work done by the system on the surroundings is δW. If P is the external pressure and f is the external force of elongation

$$\delta W = PdV - fdL \tag{1.2}$$

If the process is reversible, $\delta Q = TdS$ where S is the entropy of the elastic body. If we substitute this expression for δQ in equation 1.1 will require δW to represent the element of reversible work. In order to be able to comply with this requirement, the coefficients P and f in Eq. 1.2. must be assigned their equilibrium values. Especially, f will represent the equilibrium force for a given state of the system which may be specified variously by S, V, and L, by T, V, and L, or by T,P, and L. Then,

$$dE = TdS - PdV + fdL \tag{1.3}$$

When the Gibbs free energy is introduced

$$G = H - TS = E + PV - TS \tag{1.4}$$

Where H is the heat content of the body; $H = E + PV$

$$dG = dE + PdV + VdP - TdS - SdT \tag{1.5}$$

and substituting for dE from Eq. 1.3, it is obtained

$$dG = VdP - SdT + fdL \tag{1.6}$$

The differential change in free energy in terms of the independent variables P, T, and L can be expressed with this equation P, T and L are experimentally measurable quantities. It follows from Eq. 1.6 that

$$\left(\frac{\partial G}{\partial L}\right)_{T,P} = f \tag{1.7}$$

or

$$f = \left(\frac{\partial H}{\partial L}\right)_{T,P} - T\left(\frac{\partial S}{\partial L}\right)_{T,P} \tag{1.8}$$

The condition for an ideal elastomer is that

$$\left(\frac{\partial H}{\partial L}\right)_{T,P} = 0 \tag{1.9}$$

so,

$$f = -T\left(\frac{\partial S}{\partial L}\right)_{T,P} \tag{1.10}$$

The negative sign means that work is done on the specimen to increase its length. Similarly,

$$S = -\left(\frac{\partial G}{\partial T}\right)_{P,L} \tag{1.11}$$

Alternatively, Helmholtz free energy can be introduced defined by the relation [4];

$$A = E - TS \tag{1.12}$$

For a change taking place at constant temperature we have then

$$\delta A = dE - TdS \tag{1.13}$$

Combining this equation with Eq 1.3 we obtain the standard thermodynamic result

$$\delta A = \delta W \quad \text{(Constant T)} \tag{1.14}$$

It means that the change in Helmholtz free energy is equal to the work done on the system by the applied forces in a reversible isothermal process. Work done by the applied stress corresponding to a tensile force F acting on a specimen of length L, in this case the work done is due to a small displacement is

$$\delta W = fdL \tag{1.15}$$

By making use of Eq 1.14 and 1.15

$$f = \left(\frac{\partial W}{\partial L}\right)_T = \left(\frac{\partial A}{\partial L}\right)_T \tag{1.16}$$

which shows that the tensile force is due to change in Helmholtz free energy per unit increase in length of the specimen. The force, like the free energy, can be given as the sum of the two terms from the Eq. 1.13, thus

$$f = \left(\frac{\partial A}{\partial L}\right)_T = \left(\frac{\partial E}{\partial L}\right)_T - T\left(\frac{\partial S}{\partial L}\right)_T \tag{1.17}$$

where, the first terms expresses the change in internal energy and the second term expresses the change in entropy, per unit increase in length. Eq. 1.12 can be written in differential form

$$\delta A = dE - TdS - SdT \tag{1.18}$$

From Eq.1.3 and Eq.1.15

$$dE = fdL + TdS \tag{1.19}$$

Combining these two equations gives

$$\delta A = fdL - SdT \tag{1.20}$$

By partial differentiation

$$\left(\frac{\partial A}{\partial L}\right)_T = f \qquad \left(\frac{\partial A}{\partial T}\right)_L = -S \tag{1.21}$$

Thermo elastic experiments can be used for the explanation of the molecular origin of the elastic force f exhibited by a deformed elastomeric network. This involves the temperature dependence of either the force f at constant length L or the length at constant force. Consider first a thin metal strip stretched with a weight M to a point short of that giving permanent deformation, as is shown Figure 1.1.

The usual behavior that would be considered is the increase in length of the stretched strip as the temperature increases (at constant load). Exactly the opposite result, shrinkage, is observed in the case of a stretched elastomer. For comparison purposes, the result observed for a gas at constant pressure is included in the Figure 1.1. Raising its temperature would of course cause an increase in its volume V, as illustrated by the well-known equation PV=nRT

1. Metal

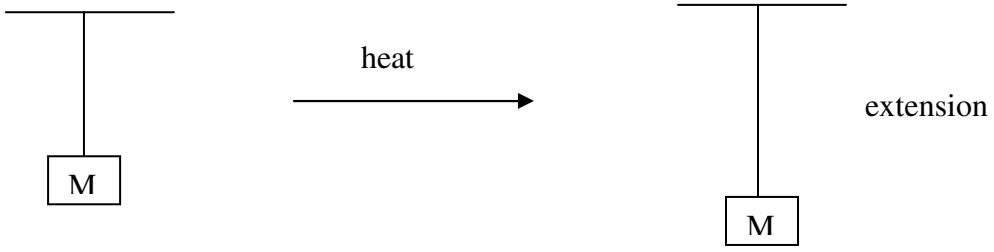

2. Rubber

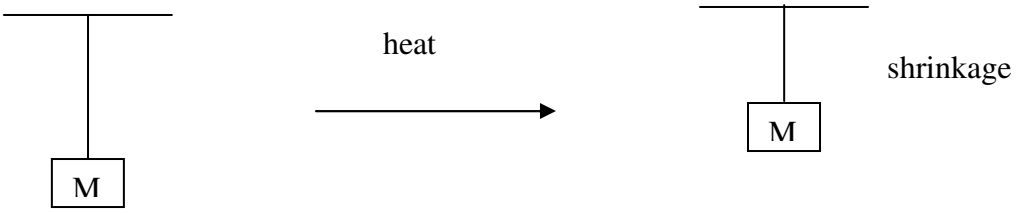

3. Gas

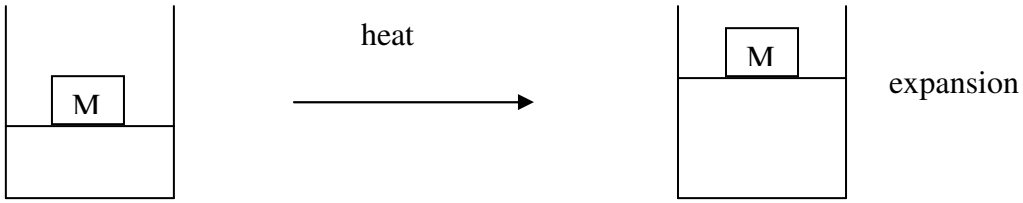

Figure1.1 Results of thermo elastic experiments carried out on a typical metal rubber, and gas [8, p.7]

The primary effect that is observed when the metal is stretched is the increase ΔE in energy caused by changing the values of the distance d of separation between the metal atoms. Upon removal of the force, the stretched strip returns back to its original dimension since this is associated with a decrease in energy. Similarly, at constant force heating the strip gives rise to the usual expansion due to the increased oscillations about the minimum in the asymmetric potential energy curve. In the case of the elastomer, however, the major effect of the deformation is stretching out of the network chains, which substantially reduces their entropy. The retractive force is the result of the tendency of the system to increase its entropy toward the maximum value that it had in the underformed state. The chaotic molecular motions of the chains are increased when the temperature is increased and thus the tendency toward the more random state increases. As a result, length is decreased at constant force, or force is increased at constant length.

1. Metal

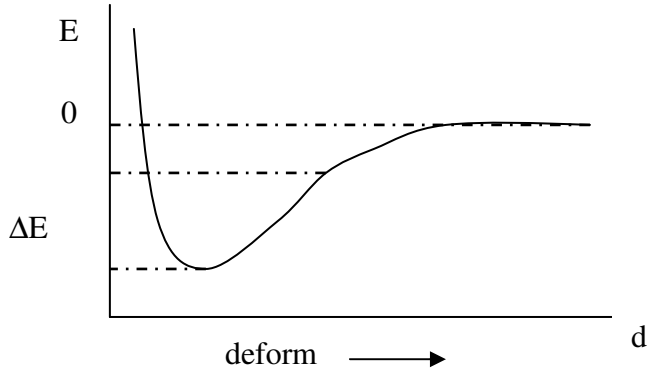

Energetically derived elasticity

2. Rubber

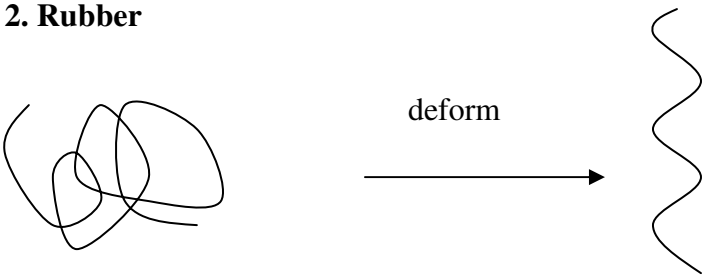

Entropically derived elasticity

3. Gas

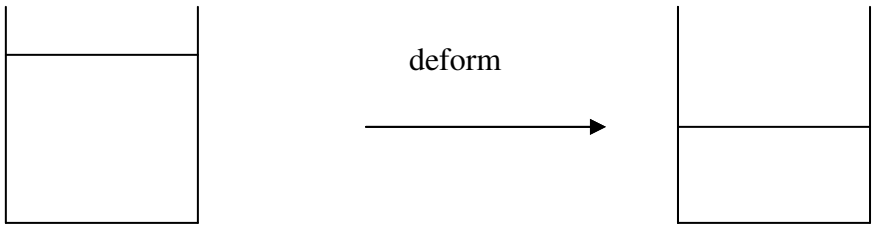

Entropically derived elasticity

Figure 1.2 Sketches explaining the observations described in Figure 1.1 in terms of molecular origin of the elastic force or pressure [8, p.7]

Elastomers also exhibit compressive recovery, unless the compressive elastic limit is not exceeded. This is called resilience. When the material is compressed, the molecules are forced into a more ordered state rather than the preferred, random state. Therefore, entropy is decreased by the compression and, on the removal of compressive force, the entropy will tend to increase again. The molecules push against the surface to be able to return to their chaotic positions again. [5]

1.2 General Approach to Rubber Elasticity

The continuum mechanical derivation of constitutive equations for elastomeric compounds is based on the concept of a strain energy density function or elastic potential Z, corresponding to the change in Helmholtz free energy of the material upon deformation [6]. It is supposed throughout that the material is isotropic and homogeneous, and that the temperature remains constant. Two approaches are generally considered for the rubber isothermal mechanical characterization: the kinetic theory which is based on the statistical thermodynamics considerations, and the phenomenological approach which treats the material as a continuum regardless of its microstructure and molecular nature. The kinetic theory dates back to 1940s. It attempts to derive elastic properties from some idealized model of the structure of vulcanized rubber. This theory, which is one of the cornerstones of our understanding of the macromolecular nature of rubber, is based on the observations that the rubber elastic deformation arises almost entirely from the decrease in entropy with increase in the applied extension. It generally deals with the assumed statistical distributions of the lengths, orientations and structure of rubber molecular networks. People have built networks from chains described by Gaussian statistics, that is the chain never approach their fully extended length, or have modified the chain statistics to allow larger stretches than are afforded by the Gaussian chain, then incorporated non-Gaussian chains into networks of three, four or eight number of chains.

Following Rivlin, phenomenological approach starts with the basic assumptions that the material is isotropic and its isothermal elastic properties may be described in terms of a strain energy function Z. Numerous strain energy density functions have been proposed, and can be subdivided according to whether Z is expressed as a polynomial function of strain invariants, or directly in terms of principle stretch ratios, and whether incompressibility is assumed or not.

1.3 The Molecular Basis of the Rubberlike Elasticity

Rubberlike materials contain long polymeric chains having a high degree of flexibility and mobility. They are joint into a network structure. The flexibility and mobility comes from the very high deformability. Because of an externally applied stress, the long polymeric chains may change their configurations, as a result of this, because of the high chain mobility an adjustment which takes place relatively rapidly within the network. Because of the solid like features in network structures chains are prevented from flowing relative to each other under external stresses. As a result of this, a rubber material can be stretched at least 2-3 times its original length. Upon removal of the external force applied, this material rapidly recovers its original dimensions, with essentially no non-recoverable strain. As a result of these mechanical properties, rubbers find important usage ranging from automobile cars to gaskets in jet planes, and space vehicles [7].

In most of the solids such as crystalline or amorphous glassy materials, when a force externally applied, it changes the distance between neighboring atoms which results in interatomic or intermolecular forces. In these materials, for the deformation to be recoverable the distance between two adjacent atoms should be changed by only about a few angstroms. When the deformations are higher, the atoms slide past each other, there may be a flow or the fracture can take place. On the other hand, the rubber response is almost entirely intra-molecular. Through the cross-links, the forces externally applied are transmitted to the long chains, change the conformations of the chains, and each polymeric chain acts like a spring in response to the external stress.

The rubberlike elasticity should be defined and then the molecular characteristics required to achieve the very unusual behavior should be described [8]. This is shown in Table 1.1

The definition of rubberlike elasticity basically has two parts (i) Very high deformability upon externally applied force and (ii) almost complete recoverability upon removal of the externally applied force. Besides these, three molecular requirements must be met for a material to exhibit this type of elasticity, as well: (i) the material must consist of polymeric

chains, (ii) the chains must have a high degree of flexibility and mobility, and (iii) the chains must form a network structure.

Table 1.1 Definition and Molecular requirements for Rubberlike Elasticity

Two Part Definition	Molecular requirement
1. Very high deformability	1. Material composed of molecules that are of i. long chains (polymers) ii. high flexibility and mobility
2. Essentially complete recoverability	2. Network structure from cross-linking of molecules

The first requirement is related to the very high deformability. It comes from the fact that the molecules in an elastomeric material should be able to change their arrangements and extensions in three dimensional spaces dramatically as a result of an externally applied stress, and only long polymeric chains have the required huge number of spatial arrangements of very different extensions. The very high deformability is also responsible from the second characteristics of rubberlike elasticity. It denotes that the chains should be flexible and mobile and as a result the different spatial arrangements of the chains should be accessible. That is to say that, the probable changes in these arrangements should not be hindered by following constraints as may result from inherent rigidity of the chains, or by decreased mobility as would result due to the chain crystallization, or from the very high viscosity characteristic of the glassy state. The network structure is obtained when the chains are joint together, or cross-linking, the segments between the cross-links, approximately one out of every 100, prevents the stretched polymeric chains from irreversibly sliding by one another. The cross-links may be either chemical bonds or physical aggregates [8].

1.4 Basic Postulates of Rubberlike Elasticity

There are two postulates which are very important for the development of molecular theories of rubberlike elasticity [8]. The first one is

i. Although there are intermolecular interactions in the rubberlike materials, these interactions are independent of configuration. In other words, they are assumed to be independent of extent of deformation and assumed play no role in deformations carried out at constant volume and composition, strain induced crystallization is the exception.

The meaning of the first postulates is that rubberlike elasticity is an intra-molecular effect, more specifically the entropy-reducing orientation of network chains. These chains should be random in the amorphous state, without any deformation. Because intermolecular effects are not dependent on intra-molecular effects, there is no inducement for the spatial configurations of the chains to be changed.

This assumption is now supported by a variety of results. First, thermo elastic results are found to be independent of network swelling. Second, neutron scattering studies have confirmed that chains in the bulk, amorphous, undeformed state are random.

The second postulate is very closely related to the first. It states:

ii. The Helmholtz free energy of the network should also be separable:

$$A = A_{liq}(T,V,N) + A_{el}(y) \tag{1.22}$$

where y is the strain tensor

It is thus assumed that the non-elastic (liquidlike) part of the network free energy is independent of deformation.

1.5 Structure of Networks

A network chain that is a chain between two junction points in fact consists of the basis of the basic molecular theory of amorphous polymeric networks. Generally, network chains have a distribution of molecular weights about an average molecular weight, which is the basis of the representative reference quantity in describing network structure. The number of chains connecting at each cross-link (or junction) is called the functionality θ of that junction. A network may consist of two or more sets of junctions with different functionalities; then we talk about an average functionality. If a chain is connected to a junction at only one end is called a dangling chain, and if both of its ends connected to the same junction is called a loop. A network is called a perfect network if it has no dangling chains or loops and all junctions have functionality greater than 2. Although it is very difficult to have a perfect network in reality, it is the simple reference structure for the molecular theories.

With the help of some parameters a perfect network may be described: the average molecular weight between junctions M_e; the number of junctions μ; the number of network chains ν; the average functionality θ; and the cycle rank ξ, which denotes the number of chains that have to be cut in order to reduce the network to a tree with no closed cycles [7,8]. These five parameters are related by three equations.

The first relation is between ν and μ. The number of the chain ends, 2ν, must be equal to the number of functional groups, $\theta\mu$, for the network to be perfect. Thus,

$$\mu = 2\nu/\theta \tag{1.23}$$

which means that, for instance, only $\mu = \nu/\theta$ junctions are required to get ν chains in a perfect tetra-functional network. This can be seen pictorially from the sketches given in Figure 1.3

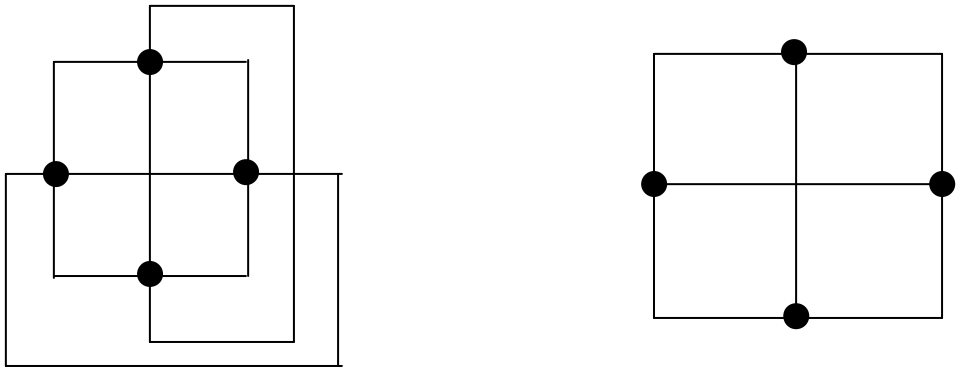

(a) (b)

Figure 1.3 Sketches of some simple, perfect networks having a) tetra-functional b) tri-functional cross-links [8, p.27]

In the tetra-functional network in Figure 1.3-a, the eight network chains should contain four junctions. On the other hand, the six chains in the tri-functional network shown in Figure 1.3-b require the same number of junctions, since the conversion factor 2/θ is now two-thirds instead of one-half.

The other equations are

$$\xi = (1 - 2/\theta)\nu \tag{1.24}$$

$$\xi / V_0 = \frac{(1 - 2/\theta)\rho}{M_c / N_A} \tag{1.25}$$

where V_0 is the volume of network, ρ is the density, and N_A is Avagadro's number.

1.6 Elasticity of the Single Chain

The sum of the elastic free energies of the individual chains consists of the elastic free energies of the network, which is indicated in the basic postulate of elementary molecular theories of rubber elasticity [7].

The statistical properties of a polymer chain are determined by its chemical structure, such as its average dimensions in space and its flexibility. They result in affecting the various properties of a network consisting of these chains. Therefore understanding of the single chain is important.

According to the statistical mechanical assumptions, when the chain is stretched from its two ends, the number of each type of isomeric state in a chain remains essentially the same. The change in the end-to-end vector occurs by the redistribution of the isomeric states along the chain. Because there is no change in the number of each type of isomeric state, during stretching, the total internal energy of the chain remains constant. The elasticity of the chain coming from redistribution of isomeric states is called as entropic elasticity, and a major part of the elasticity of a network is entropic. During deformation if part of the work done is used to change relative populations of isomeric states, the bond angles, and the chain lengths, a change in internal energy takes place which results in an "energetic" component of the elasticity.

The vector r takes different values resulting from rotations about the individual bonds. For chains with more than about 50 skeletal bonds, the probability P(r)dxdydz that one end of r is at the origin and the other end is an infinitesimal volume dV=dxdydz is given by the Gaussian function

$$P(r)dxdydz=(3/2\pi\langle r^2\rangle_0)^{3/2} \exp(-3\, r^2/2\langle r^2\rangle_0)dxdydz \qquad (1.26)$$

Here $\langle r^2\rangle_0$ is the average of the squared end to end vectors, and the subscribed zero indicates that the chain is in the unperturbed or so called theta state. It is now indicated that chains in the bulk undiluted state are in the unperturbed state. Eq.1.26 represents the probability distribution of the vectorial quantity r. The distribution p(r) showing the

probability is that the magnitude r of r has a certain value irrespective of the direction. Thus, the probability that the end to end length of the chain is in the range r to r + dr irrespective of its direction is

$$p(r)dr = (3/2\pi\langle r^2\rangle_0)^{3/2} \exp(-3\, r^2/2\langle r^2\rangle_0) 4\, \pi\, r^2\, dr \qquad (1.27)$$

The thermodynamic expression which relates the elastic free energy A_{el} of a Gaussian chain to the probability distribution P(r) is

$$A_{el} = C(T) - kT \ln P(r) \qquad (1.28)$$

where C(T) is a function of temperature T, and k is the Boltzmann constant. Substituting Eq. 1.26 into 1.27 leads to

$$A_{el} = A^*(T) + (3kT/2\langle r^2\rangle_0) r^2 \qquad (1.29)$$

Here, $A^*(T)$ is a function of temperature alone. Eq. 1.29 is the elastic free energy of a Gaussian chain with two ends fixed at a separation of r. The average force which is required to keep the two ends at this length from each other is obtained from the thermodynamic expression

$$f = \left(\frac{\partial A_{el}}{\partial r}\right)_T \qquad (1.30)$$

$$= \left(\frac{3kT}{\langle r^2\rangle_0}\right) r \qquad (1.31)$$

where Eq.1.31 is obtained by substituting Eq. 1.29 into Eq. 1.30. The subscript T denotes that temperature is constant.

Equation 1.31 states that the single chain acts as a spring with spring constant $3kT/\langle r^2\rangle_0$.

1.7 Elasticity of the Network

Since there are ν chains in the network, the total elastic free energy ΔA_{el} of the network relative to the undeformed state is obtained by summing Eq. 1.29 [7].

$$\Delta A_{el} = \frac{3kT}{2\left\langle r^2 \right\rangle_0} \sum_{\upsilon} \left(r^2 - \left\langle r^2 \right\rangle_0 \right) \tag{1.32}$$

$$= \frac{3\upsilon kT}{2} \left(\frac{\left\langle r^2 \right\rangle}{\left\langle r^2 \right\rangle_0} - 1 \right) \tag{1.33}$$

where $\left\langle r^2 \right\rangle = \sum r^2 / \upsilon$ is the average square of the end to end vectors of chains in the deformed network. Substituting

$$\left\langle r^2 \right\rangle = \left\langle x^2 \right\rangle + \left\langle y^2 \right\rangle + \left\langle z^2 \right\rangle \tag{1.34}$$

in Eq. 1.33 and knowing that chain dimensions are isotropic in the undeformed state i.e.

$$\left\langle x^2 \right\rangle_0 = \left\langle y^2 \right\rangle_0 = \left\langle z^2 \right\rangle_0 = \left\langle r^2 \right\rangle_0 / 3 \tag{1.35}$$

one gets

$$\Delta A_{el} = \frac{\upsilon kT}{2} \left[\frac{\left\langle x^2 \right\rangle}{\left\langle x^2 \right\rangle_0} + \frac{\left\langle y^2 \right\rangle}{\left\langle y^2 \right\rangle_0} + \frac{\left\langle z^2 \right\rangle}{\left\langle z^2 \right\rangle_0} - 3 \right] \tag{1.36}$$

The x, y and z coordinates shown in the above equations are the laboratory fixed coordinates.

The ratios seen in Eq. 1.36 are microscopic quantities. To be able to define the elastic free energy of a network according to the macroscopic state of deformation, an assumption which relates the microscopic chain dimensions to macroscopic deformation has to be made.

The state of macroscopic deformation may be characterized by extension ratios along the x, y and z directions, respectively as

$$\lambda_x=L_x/L_{x0} \ , \lambda_y=L_y/L_{y0} \ , \quad \lambda_z=L_z/L_{z0} \tag{1.37}$$

where L_{x0}, L_{y0}, L_{z0} are the lengths before deformation and L_x, L_y, L_z are the corresponding lengths in the deformed state.

Two basic network models to relate the microscopic deformation to the macroscopic deformations are: the affine network and the phantom network.

1.7.1 The Affine Network Model

The Affine network model is based on the following fundamental assumptions [9];

i. The network consists of ν freely jointed Gaussian chains, where such a network chain is defined as a sequence of skeletal bonds lying between two junctions. The mean square end-to-end dimensions of the ensemble of network chains in the undeformed network are the same as those for an ensemble of chains in the bulk, uncross-linked state. The mean end-to-end dimensions of the latter, in turn, are equal to those of the single chain in the unperturbed state.

ii. There is no change in volume upon deformation

iii. The junctions move affinely with macroscopic deformation. This assumption played a central role in theories of rubberlike elasticity until neutron scattering experiments showed that the junctions are not rigidly embedded in the network and that their departure from affine displacement is substantial. It should be noted that the affine assumption suppresses the flu actuations of he chain end points, but does not impose any constraints at points along the

chain contour. In this respect, the chains do not interact with their environments along their contour.

iv. The total elastic energy of the network is the sum of the elastic energies of the individual chains. Due to assumption that the chains are freely jointed, all spatial arrangements are of the same energy, the network deformation is purely entropic, and the relation $\Delta A_{el} = \Delta E - T\Delta S$ becomes $\Delta A_{el} = -T\Delta S$. The treatment may be generalized to non-freely-jointed chains, however.

The elastic free energy of an isolated deformed Gaussian chain with its two ends fixed at r is given as

$$A(r) = A(T) + \frac{3kT}{2\langle r^2 \rangle_0} r^2 \tag{1.38}$$

Since there are many chains, this equation should be summed for all chains of the network, and then the change ΔA_{el} in the total elastic energy at constant temperature (relative to that of undeformed state) is obtained as

$$\Delta A_{el} = \frac{3kT}{2\langle r^2 \rangle_0} \sum_{\upsilon} \left(r^2 - \langle r^2 \rangle_0 \right) \tag{1.39}$$

$$= \frac{3}{2} \upsilon kT \left(\frac{\langle r^2 \rangle}{\langle r^2 \rangle_0} - 1 \right)$$

From the first equality to the second equality in Eq. 1.38, the relationship $\langle r^2 \rangle = \sum_{\upsilon} r^2 / n$ is used to represent the average of the squared end-to-end vectors. When we write the end-to end vector according to the Cartesian components and when we average over the ensemble of chains gives;

$$\langle r^2 \rangle = \langle x^2 \rangle + \langle y^2 \rangle + \langle z^2 \rangle \tag{1.40}$$

When we divide the both sides of this equation by $\langle r^2 \rangle_0$ knowing that the network chains are isotropic in the undeformed state, and using the assumption that the chain ends are displaced proportionally to the macroscopic strain, results in;

$$\langle r^2 \rangle / \langle r^2 \rangle_0 = \left(\lambda_x^2 + \lambda_y^2 + \lambda_z^2\right)/3 \tag{1.41}$$

Here, λ_x, λ_y and λ_z are the elements of the deformation tensor y, and can be defined as the ratio of the final length to the initial length, in all coordinate direction. Substitution of Eq. 1.41 into Eq. 1.38 gives,

$$\Delta A_{el} = (1/2)\upsilon kT\left(\lambda_x^2 + \lambda_y^2 + \lambda_z^2 - 3\right) \tag{1.42}$$

Here it is pointed out that the intermolecular interactions are accepted as zero in this model, that is, the system is essentially like an ideal gas. Then the expression for the force f is obtained from the thermodynamic expression;

$$f = \left(\frac{\delta \Delta A_{el}}{\delta L}\right)_{T,V} = L_0^{-1}\left(\frac{\delta \Delta A_{el}}{\delta \lambda}\right)_{T,V} \tag{1.43}$$

where $\lambda = \lambda_x = L/L_0$ The assumption here made is that the volume of the sample remains constant during deformation, and the y and z components of the deformation are written as $\lambda_y = \lambda_z = \lambda^{-1/2}$. Substituting Eq. 1.42 into 1.43 and after differentiation the elastic equation of state for the force is;

$$f = \left(\frac{\upsilon kT}{L_0}\right)\left(\lambda - 1/\lambda^2\right) \tag{1.44}$$

It should be pointed out that although the model assumes the simple additivity of the free energies of the individual chains and disregarding the intermolecular interactions, its predictions well suit to the experimental data within reasonable limits.

1.7.2 The Phantom Network Model

In terms of the phantom network model, the junction points fluctuate as the time passes but, neighboring chains do not have effect on them. The macroscopic state of deformation does not affect the extent of fluctuations. The term phantom is coming from the assumed ability of the junctions to fluctuate despite of their entanglements with network chains. The assumptions for this model are given as follows [7-9];

i. The network chains are Gaussian

ii. Some of the junctions at the surface of the networks are fixed and deform affinely with macroscopic strain

iii. The chains are subject only to constraints that arise directly from the connectivity of the network. The effects of junctions and chains on one another are of no consequence, and the effect of the macroscopic strain is transmitted to a chain through the junctions to which a chain is attached at its two ends. This characteristic of a phantom network holds at all deformations.

In terms of the theory, a small part of the junctions are assumed to be fixed at the surface of the network, and most of the junctions are free to fluctuate over time. The instantaneous end-to-end vector of each chain may be represented as a sum of a $\bar{r}_i$ and a fluctuation Δr_i from the mean

$$r_i = \bar{r}_i + \Delta r_i \tag{1.45}$$

The subscript i signifies that Eq.1.45 is for the i^{th} chain.

The dot product of both sides of Eq.1.45 is

$$r_i^2 = \bar{r}_i^2 + 2\bar{r}_i.\Delta r_i + (\Delta r_i)^2 \tag{1.46}$$

When we average both sides of Eq.1.46 for all chains of the network in the undeformed state and in the deformed state gives

$$\left\langle r^2 \right\rangle_0 = \left\langle \bar{r}^2 \right\rangle_0 + \left\langle (\Delta r)^2 \right\rangle_0 \tag{1.47}$$

$$= \left\langle \bar{x}^2 \right\rangle_0 + \left\langle \bar{y}^2 \right\rangle_0 + \left\langle \bar{z}^2 \right\rangle_0 + \left\langle (\Delta x)^2 \right\rangle_0 + \left\langle (\Delta y^2) \right\rangle_0 + \left\langle (\Delta z^2) \right\rangle_0$$

The average of the term $\bar{r}_i.\Delta r_i$ in Eq.1.46 is zero since fluctuations of chain dimensions are uncorrelated with mean chain vectors.

At any given time, the mean position $\bar{r}$ and fluctuations Δr shows distributions that may be assumed to be Gaussian. The mean squared values $\left\langle \bar{r}^2 \right\rangle_0$ and $\left\langle (\Delta r)^2 \right\rangle_0$ are related to $\left\langle r^2 \right\rangle$ according to the theory by

$$\left\langle \bar{r}^2 \right\rangle_0 = \left(1 - \frac{2}{\phi}\right) \left\langle r^2 \right\rangle_0 \tag{1.48}$$

$$\left\langle (\Delta r)^2 \right\rangle_0 = \frac{2}{\phi} \left\langle r^2 \right\rangle_0 \tag{1.49}$$

The components of mean position $\bar{r}$ of each chain deforms affinely with macroscopic deformation while fluctuations Δr are not affected;

$$\left\langle \bar{x}^2 \right\rangle = \lambda_x^2 \left\langle \bar{x}^2 \right\rangle_0, \quad \left\langle \bar{y}^2 \right\rangle = \lambda_y^2 \left\langle y^2 \right\rangle_0, \left\langle \bar{z}^2 \right\rangle = \lambda_z^2 \left\langle \bar{z}^2 \right\rangle_0 \tag{1.50}$$

$$\left\langle (\Delta x)^2 \right\rangle = \left\langle (\Delta x)^2 \right\rangle_0, \quad \left\langle (\Delta y)^2 \right\rangle = \left\langle (\Delta y)^2 \right\rangle_0, \quad \left\langle (\Delta z)^2 \right\rangle = \left\langle (\Delta z)^2 \right\rangle_0 \tag{1.51}$$

Substituting Eq. 1.50 into Eq. 1.47 and using Eq.1.48 and 1.49 and the condition of isotropy in the state of rest leads to

$$\left\langle r^2 \right\rangle = \left[\left(1 - \frac{2}{\phi} \right) \frac{\lambda_x^2 + \lambda_y^2 + \lambda_z^2}{3} + \frac{2}{\phi} \right] \left\langle r^2 \right\rangle_0 \tag{1.52}$$

Using Eq. 1.24 and Eq. 1.52 in 1.33 gives the following elastic free energy expression for the phantom network.

$$\Delta A_{el} = \frac{1}{2} \xi kT \left(\lambda_x^2 + \lambda_y^2 + \lambda_z^2 - 3 \right) \tag{1.53}$$

1.7.3 Comparing the Models

The affine model and phantom model differs from each other in terms of elastic free energy term in that the nature of transformations of chain dimensions built into the two models of the elementary theory.

The elastic free energy expressions for both models may be given as

$$\Delta A_{el} = \Im kT \left(\lambda_x^2 + \lambda_y^2 + \lambda_z^2 - 3 \right) \tag{1.54}$$

where the front factor $\Im$ is equal to $\upsilon/2$ for the affine network model and to $\xi/2$ for the phantom network model. For a perfect tetra-functional network, $\Im$ for the latter model is half the value for the former.

The simplified elastic free energy for the Affine network model deviates from that obtained by Flory [8]. Since, there is an additional logarithmic term which is a gas-like contribution due to the distribution of the cross-links over the sample volume. Thus the correct expression for the elastic free energy of the affine network model is

$$\Delta A_{el} = \frac{\upsilon kT}{2} \left(\lambda_x^2 + \lambda_y^2 + \lambda_z^2 - 3 \right) - \mu kT \ln \left(\frac{V}{V_0} \right) \tag{1.55}$$

where V is the final volume of the network.

The most important thing of the molecular theory of rubber elasticity is to make a correlation between the state of deformation at the molecular level and the externally applied macroscopic deformation. The affine and phantom network models are two simplest models derived for this aim. In the affine network model, it is assumed that the junctions are embedded securely in the network structure. They do not show any fluctuations over time as would be observed in a real network whose junctions show rapid fluctuations about their mean positions. As a conclusion of the junctions embedded in the network, the junctions translate affinely with macroscopic strain. There is no assumption with regard to the parts of a chain between its junctions. On the other hand, the junction points in the phantom network model reflect the full mobility of the chains subjects only to the effects of the connectivity of the network. The position of a junction can be determined according to a time averaged mean location and instantaneous fluctuations from it. In terms of this opposite case, the mean locations of junctions transform affinely with macroscopic deformation, whereas the instantaneous fluctuations are not affected from this macroscopic deformation. It is the phantomlike nature of the chains that they are independent of the instantaneous fluctuations from the macroscopically applied state of deformation. During these fluctuations the chains may pass freely through each other. They are unaffected by the volume exclusion effects of neighboring chains and therefore by the macroscopically applied deformation [8].

1.8 Constrained Junction Model

The affine and phantom networks given above are based on a hypothetical chain which may pass freely through its neighbors as well as through itself. [9]. However, in a real chain the situation is different. The volume of a segment is excluded to other segments belonging either to the same chain or to others in the network. As a result, the uncrossability of chain contours by those occupying the same volume becomes an important factor. Uncross-linked bulk polymer contains highly entangled chains. During formation of the network these entanglements are permanently fixed when the chains are joined. The number of chains sharing the volume occupied by a given chain has a close relation to the degree of entanglement or the degree of interpenetration in a network. Deformation dependent

contributions from entanglements can be best seen in decreasing in network modulus with increasing tensile strain or swelling. The constrained junction model is based on the assumption that, when the polymer is stretched the space available to a chain along the direction of stretch is increased, thus resulting in an increase in the freedom of the chain to fluctuate. In the same manner, when a polymer swells in a good solvent then the separation of the chains from one another increases, resulting in decreasing their correlations with neighboring chains. The starting point of the constrained junction model is the elastic free energy as it is stated for the other models. In agreement with experimental observations, there are two contributions for this model in the deformed network for free energy, one from the phantom network and the other from the entanglements. There are two assumptions for this theory given as the following [9]

i.The network is of uniform structure

ii.The entanglement constraint about every junction is the same

A real network, indeed, shows the properties between that of the affine and the phantom network models. In this model, junction fluctuations occurs but not to the extent in the phantom model. Constrained junction model is a model which is a quantitative model of a network with fluctuations of junctions dependent non-affinely on the macroscopic state of strain. In terms of this model, the fluctuations of junctions are affected by the copious interpenetration of their pendent chains with the spatially neighboring junctions and chains. The most important thing is the degree of interpenetration of a chain with its environment. This is described schematically for a tetra-functional network in Figure 1.4-a [8] where four filled circles are the junctions that are topologically neighbors of a given junction (empty one)

The spatially neighboring junctions are shown by X's. The average number Γ of junctions within this domain is given by

$$\Gamma = \frac{4\pi}{3}\left\langle r^2 \right\rangle_0^{3/2} \frac{\mu}{V_0} \tag{1.56}$$

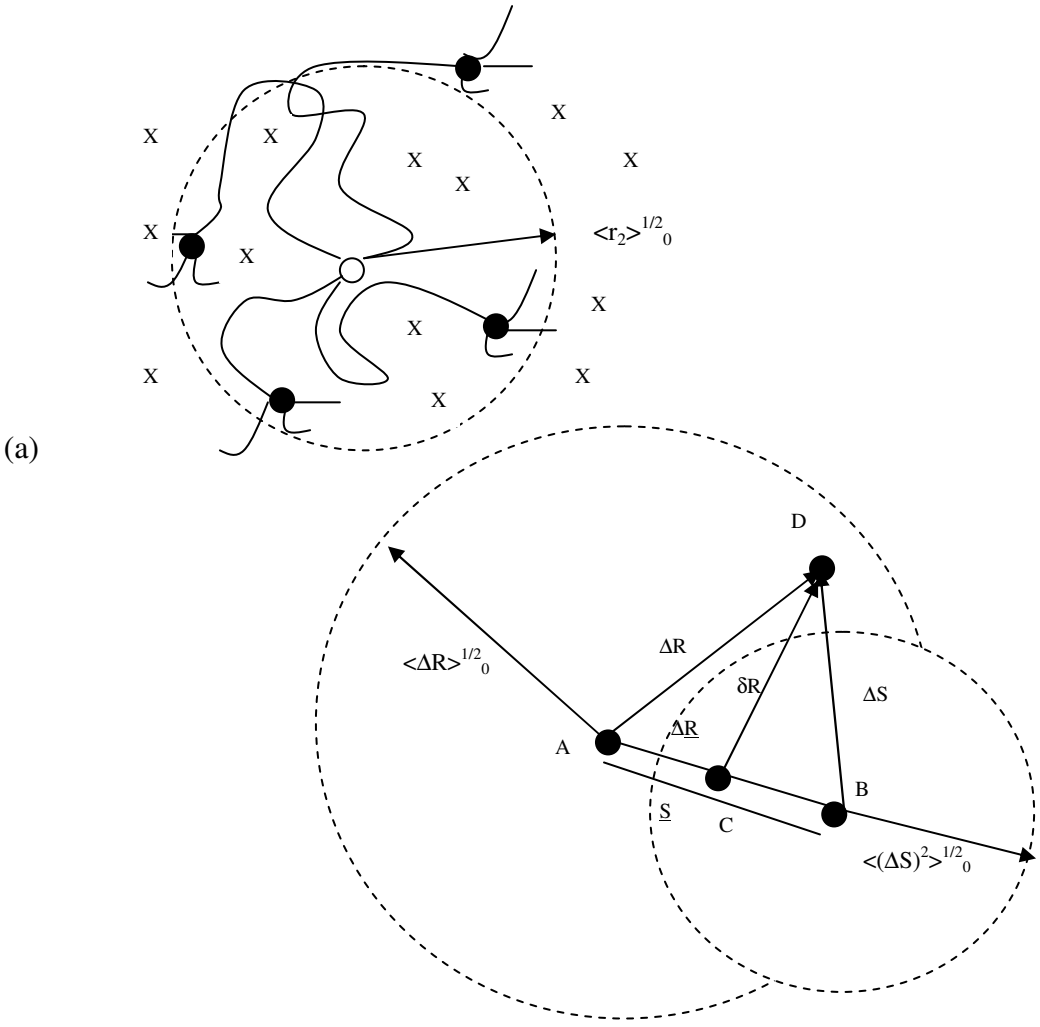

Figure 1.4 a) Figure showing tetrafunctional junction (empty circle) surrounded by spatial neighboring junctions (X's) and four topological junctions (filled circles) b) Various variables defining the mean and instantaneous positions of a given junction in the phantom network [8, p.37]

where $\frac{\mu}{V_0}$ is the number of junctions per unit volume in the reference state of the network. Generally Γ is in the range of 25-100 in typical networks. When the macroscopic deformation is applied, a significant degree of rearrangement of junctions in domain shown by the dashed circle is expected to occur unlike the limiting case of the phantom networks.

A junction point in the constrained junction network model got affected from the phantom network and the constrained domains, as shown in Figure 1.4-b. Point A is the mean position of the junction in the phantom network. The large dashed circle of radius $\left\langle (\Delta R)^2 \right\rangle_{ph}^{1/2}$ is the root mean square of the fluctuation domain for the given junction in the phantom network. Point B is the mean location of constrains. It is at a distance $\bar{s}$ from the phantom center. The small dashed circle of radius $\left\langle (\Delta s)^2 \right\rangle_0^{1/2}$ is the root mean square size of the constrained domain in which the junction would fluctuate under the effect of constraints only. Point C is the mean position of the junction which is affected from the phantom network and constraints. Point D is the instantaneous location of the junction at a distance of ΔR, Δs, δR from points A, B and C, respectively. A quantitative measure of the strengths of the constraints is given by the ratio

$$\kappa = \left\langle (\Delta R)^2 \right\rangle_{ph} / \left\langle (\Delta s)^2 \right\rangle_0 \tag{1.57}$$

If there is no constraints action $\left\langle (\Delta s)^2 \right\rangle_o \longrightarrow \infty$ and $\kappa = 0$ from Eq.1.57. In this case we end up with the phantom limit. On the other hand, if constraints are infinitely strong then there is no junction fluctuations, then $\left\langle (\Delta s)^2 \right\rangle_o \longrightarrow 0$ and $\kappa \longrightarrow \infty$. In this case we end up with the affine limit.

The elastic free energy of the network is obtained as the sum of the phantom network and constrained free energies, ΔA_{ph} and ΔA_c:

$$\Delta A_{el} = \Delta A_{ph} + \Delta A_c \tag{1.58}$$

where the phantom network elastic energy is given by Eq.1.53. The elastic free energy change because of the constraints can be given according to the components of the principle extension ratios:

$$\Delta A_c = \frac{1}{2} \mu kT \sum_t \left[B_t + D_t - \ln(B_t + 1) - \ln(D_t + 1) \right] \text{ t=x,y,z} \tag{1.59}$$

where

$$B_t = \kappa^2\left(\lambda_t^2 - 1\right)\left(\lambda_t^2 + \kappa\right)^{-2}, \quad D_t = \lambda_t^2 \kappa^{-1} B_t \tag{1.60}$$

The constrained junction model formulations are based on determination of the distribution of fluctuations δR from the mean position of the junction which is affected by the phantom network and constrained effects in the deformed network [10-12]. Since when $\kappa = 0, \Delta A_c = 0$ the elastic free energy of the network is equal to that of the phantom network and as κ increases indefinitely, the elastic free energy converges to the affine network, the constrained junction model is a network with elastic free energy intermediate in value between the phantom and the affine network limits. The affine network model describes the real network at low deformations and the phantom network model describes the real network as the deformation increases.

The κ parameter of the constrained junction model, defined by Eq.1.57 can be interpreted in terms of the molecular constitution of the network by assuming it to be proportional to the average number of junctions in the domain occupied by a network chain. Thus;

$$\begin{aligned} \kappa &= I\left(N_A d/2\right)^{3/2}\left(\left\langle r^2\right\rangle_0 / M\right)^{3/2}\left(\xi/V_0\right)^{-1/2} \\ &= I\left(2/\phi\right)\left(N_A d\right)\left(\left\langle r^2\right\rangle_0 / M\right)^{3/2} M_c^{1/2} \end{aligned} \tag{1.61}$$

where I is the constant of proportionality, N_A is Avogadro's number, d is the network density, M is the molecular weight of a chain with end to end mean square length $\left\langle r^2\right\rangle_0$. Eq.1.61 indicates that κ is inversely proportional to the square root of cycle rank density ξ/V_0, inversely proportional to the functionality ϕ, and directly proportional to the square root of network chain molecular weight M_c.

1.9 Mooney Rivlin

As an alternative to the molecular approach of the three models described above, a phenomenological model of elasticity may be used. In such a model, a general expression for the free energy is written without asking any questions about the molecular interpretation of the terms of this free energy [13].

The model developed by Mooney and Rivlin starts from three strain invariants (they are called invariants because they are independent of the choice of coordinate system)

$$I_1 = \lambda_x^2 + \lambda_y^2 + \lambda_z^2 \tag{1.62}$$

$$I_2 = \lambda_x^2\lambda_y^2 + \lambda_y^2\lambda_z^2 + \lambda_z^2\lambda_x^2 \tag{1.63}$$

$$I_3 = \lambda_x^2\lambda_y^2\lambda_z^2 \tag{1.64}$$

The free energy density of the network F/V is written as a power series in the difference of these invariants from their values in the undeformed network ($\lambda_x = \lambda_y = \lambda_z = 1$):

$$\frac{F}{V} = C_0 + C_1(I_1 - 3) + C_2(I_2 - 3) + C_3(I_3 - 1) + \ldots \tag{1.65}$$

The second term in the series is analogous to the free energy of the classical model.

$$C_1(I_1 - 3) = C_1\left(\lambda_x^2 + \lambda_y^2 + \lambda_z^2 - 3\right) \tag{1.66}$$

With the identification $C1=G_x/2$. The third term in Eq.1.65 describes the deviations from the classical dependence. For incompressible networks, the third invariant does not change with deformation,

$$I_3 = \lambda_x^2 \lambda_y^2 \lambda_z^2 = \left(\frac{V}{V_0} \right)^2 = 1 \tag{1.67}$$

Making the fourth term of Eq.1.65 zero.

For uniaxial deformation of an incompressible network,

$$\lambda_x = \lambda \qquad \lambda_y = \lambda_z = \frac{1}{\sqrt{\lambda}} \tag{1.68}$$

the Mooney Rivlin free energy density is written in terms of the stretching factor λ :

$$\frac{F}{V} = C_0 + C_1\left(\lambda^2 + \frac{2}{\lambda} - 3 \right) + C_2\left(2\lambda + \frac{1}{\lambda^2} - 3 \right) + \ldots \tag{1.69}$$

The true stress in the Mooney Rivlin model can be obtained from the free energy density:

$$\sigma_{true} = \frac{1}{L_y L_z} \frac{\partial F}{\partial L_x} = \lambda \frac{\partial (F/V)}{\partial \lambda} = 2C_1\left(\lambda^2 - \frac{1}{\lambda} \right) + 2C_2\left(\lambda - \frac{1}{\lambda^2} \right) + \ldots$$

$$= \left(2C_1 + \frac{2C_2}{\lambda} \right)\left(\lambda^2 - \frac{1}{\lambda} \right) + \ldots \tag{1.70}$$

The engineering stress can be calculated from the true stress by:

$$\sigma_{eng} = \frac{\sigma_{true}}{\lambda} = \left(2C_1 + \frac{2C_2}{\lambda} \right)\left(\lambda - \frac{1}{\lambda^2} \right) \tag{1.71}$$

This leads to the famous Mooney Rivlin equation:

$$\frac{\sigma_{true}}{\lambda^2 - 1/\lambda} = \frac{\sigma_{eng}}{\lambda - 1/\lambda^2} = 2C_1 + \frac{2C_2}{\lambda} \tag{1.72}$$

In Mooney Rivlin equation $2C_1$ and $2C_2$ are the phenomenological coefficients which become functions of time when stress relaxation is considered [14]. The long-time relaxation experiments of Ferry et. al, [14]on lightly cross-linked poly-butadiene networks showed that the time dependent Mooney-Rivlin equation describes the slow relaxation of uniaxial stress as well, with the observation that $2C_1$ is approximately independent of time, whereas the slope $2C_2(t)$ depends on time. Thus, Eq. 1.72 serves as a good approximation both in equilibrium and out of equilibrium behavior of networks.

In molecular interpretations of rubber elasticity, the $2C_1$ intercept is generally associated with contributions from the network cycle rank proportional to the number of chains constituting the network, and the slope $2C_2$ is associated with contributions from constraints that affect the fluctuations of chains and junction points. Thus, the $2C_1$ term reflects contributions from network topology, whereas the $2C_2$ reflects effects of constraints that suppress the fluctuations in the system. If the length of a chain between two cross-links is much larger than the entanglement length represented by the entanglement molecular weight, M_e , then under sudden stretch, each sub chain of molecular weight M_e will act as a transient network chain and will contribute to the stress. The $2C_1$ will be large, reflecting these transient contributions, and will subsequently decrease upon relaxation. Thus, at shorter time scales, $2C_1$ exhibits time dependence and relaxation contains components from the transient entanglement network.

The contribution of entanglements to $2C_1$ has been the focus of both experimental and theoretical studies over the past several decades. Some experiments[15] show that at equilibrium, the effects of entanglements diminish at high extensions and/or high swelling ratios, and have no contribution to the $2C_1$ intercept, while others [16] show that contributions from chain entanglements trapped in the system during cross-linking do not relax fully and contribute to $2C_1$ [17]. The experiments of Rennar and Oppermann [18] showed the conditions under which trapped entanglements are important in a conclusive manner.

CHAPTER 2

2. BACKGROUND

In this section, the literature regarding the viscoelastic theories both molecular origin based and phenomenological based will be reviewed. The literature in relation to the stress relaxation will also be reviewed.

R.J. Spontak et al [19] worked on the stress relaxation study of the acrylate terminated urethane blends in toughened epoxies. They examined the effect of flexibilizer polydispersability on the stress relaxation behavior of a commercial epoxy. They prepared different epoxy samples containing varying compositions of acrylate terminated urethanes. They made stress relaxation tests and tried to fit the data to Kohlrausch Williams Watts or stretched exponential equation. Results were unsatisfactory since this expression cannot be used for a bimodal relaxation process. Therefore, they applied a biexponential, or two term Maxwell expression of the form,

$$\sigma_n(t)=\phi_{slow}\exp(-t/\tau_{slow}) + \phi_{fast}\exp(-t/\tau_{fast}) \qquad (2.1)$$

Fitting this equation to the data gave a good agreement. They concluded that tensile stress relaxation data from these blends are well represented by a biexponential decay expression possessing two characteristic relaxation times for fast and slow relaxation process.

Ehabe et al [20] worked on the modeling of Mooney viscosity relaxation in natural rubber. They compared the 4 different relaxation model with the experiments and made a ranking in terms of the "goodness of the fit" of the data. They used 14 samples. 12 of them are natural rubber 2 of them are synthetic polyisoprene. They used simple Mooney viscosimeter for the experiments and conducted the test at 100^0C and (1+4) minutes. (1 minute preheating

time, 4 minutes testing time) They used Maxwell model, Wu Abott model, Power law and stretched exponential model (Kohlrausch-Williams-Watts). Of the four model tested, the tri-exponential generalized Maxwell model and the Wu-Abott model proved to be the most efficient in terms of fitting the experimental data. The power law usually employed was one of the least appropriate models.

Stephan A. Baeurle et al [21] worked on a new semi-phenomenological approach to predict the stress relaxation behavior of thermoplastic elastomers. They compared their theoretical studies with the experimental test results which had been conducted by Hotta et al with poly(styrene-isoprene-styrene) tri-block copolymers. The origin of their theoretical approach was based on the studies conducted by Gurtovenko and Gotlib who described the relaxation dynamics of inhomogeneously cross-linked polymers forming agglomerations of cross-links. In this study, they demonstrated that method can be extended to predict the stretched exponential stress decay of homogeneously cross-linked thermoplastic elastomer. Their model correctly predicted the power law decay behavior, experimentally observed by Hotta et al below a characteristic temperature, by assuming a macroscopically large single domain system of cross-links. Their model correctly predicted the experimentally determined of the stretched exponential, which governs the decay behavior of the overall effective extensional modulus above characteristic temperature. Their study also demonstrated that the mechanical properties of thermoplastic elastomers are strongly influenced by multiple length and time scales.

C.K.Ober et al [22] worked on the stress relaxation of a main chain, smectic polydomain liquid crystalline elastomer. In this study they used diglycidyl ether of 4,4'-dihydroxy-α-methylstilbene as liquid crystalline elastomer. They also tested polyisoprene for the stress relaxations. They fitted data to a single stretched exponential function as described by Kohlrausch-Williams-Watt. For the epoxide based, main chain, smectic LCE, it was found that this material exhibits a large amount of stress relaxation, approximately an order of magnitude greater than amorphous, isotropic polyisoprene rubber. They have found that the relaxation moduli of the smectic LCE could be described by a stretched exponential function with a single relatively fast characteristic relaxation time (τ=60s) regardless of the magnitude of the strain. The same relaxation time was found to be as 415s for the polyisoprene elastomer.

S. Ronan et al [23] worked on the long term stress relaxation prediction for elastomer using the time temperature superposition method. They used William-Landel-Ferry (WLF) and Arrhenius plots for this study. They used NR based samples vulcanized by conventionally and semi efficiently. They measured the stress relaxation in compression mold just by thinking the application of elastomers in sealing purposes. They also examined the dynamic mechanical properties of the samples namely G' and G'' by using MTS test equipment. They shifted tan delta value which is the ratio of G'' and G' and showed that the same shift factor a_t can used for G' and G'' as well. In the stress relaxation tests conducted at different temperatures they realized that the sample vulcanized by conventionally shows different characteristics than vulcanized by semi efficiently at high temperatures. At the lower temperatures both samples showed the same stress relaxation characteristics. By using these graphs and WLF equation they shifted horizontally along the time axis by taking the reference temperature as 23 ^{0}C. They showed that both samples have produced plausible master curves to predict the 10 years or more stress relaxation. They also added that these predictions should be verified by real time tests.

Aleksey D. Drozdov and Al Dorfmann [24] studied the nonlinear viscoelastic response of carbon black filled natural rubbers. They used natural rubber compounds with 3 different carbon black loadings, namely 20-45-60 phr. They used dumbbell shaped test specimens for the relaxation tests. Their elongation ratio was changed from 2.0 to 3.5. They derived a constitutive equation and compared the experimental results with it. They modeled the filled rubber as an equivalent transient network of macromolecules. The network is assumed to be strongly heterogeneous, and it is treated as an ensemble of meso-regions with various activation energies for separation strands from temporary nodes. They introduced two types of meso domains; passive, where rearrangement of strands is prevented by surrounding chains and filler clusters, and active, where the rearrangement process is governed by the Eyring equation. There are some adjustable parameters in the stress strain relation which was found by fitting observations in relaxation tests at elongations up to 350%. The results demonstrated fair agreement with the experimental results.

A. Hotta et al [25] worked on the stress relaxation in transient networks of symmetric tri-block Styrene-Isoprene-Styrene copolymer. They used two different copolymer having 14% and 17% styrene contents. In this study they were concerned with the mechanical stress relaxation in an effective elastomer formed by the microphase separated SIS copolymer melt.

Their findings showed that the two samples under investigation show very similar mechanical relaxation despite their rather different "cross-linking morphology". The stress relaxation curves below 30^0C are essentially straight lines and parallel to each other. At a temperature around T^* 30^0C the relaxation curve deviates from this straight line (power law) behavior. In the region below 30^0C both samples have their stress relaxing according to

$$E(t) = E_0(1+1.6t^{-0.12}) \text{ for 14\% PS} \quad (2.2)$$

$$E(t) = E_0(1+2.2t^{-0.15}) \text{ for 17\% PS} \quad (2.3)$$

with only E_0 a fitting parameter. Significantly, all curves for a given material can be fitted with the same power law exponent 0.12 or 0.15 and a pre-factor of 1.6 or 2.2. At higher temperatures, above T* or equivalently at longer times on the master curves, the stress relaxation becomes much faster. From 39 to 70^0C, the stretched exponential law becomes the only reasonable model that can fit the data for both samples;

$$E(t) = 835 \exp[-(t/\tau)^{0.2}] \text{ for 4\%PS} \quad (2.4)$$

$$E(t) = 1088 \exp[-(t/\tau)^{0.2}] \text{ for 17\%PS} \quad (2.5)$$

As with the low temperature regime, all curves for a given sample can be fitted with only one fitting parameter, τ. The stretched exponent index has the same value of 0.2 for all experiment runs.

M. Van Der Horst et al [26] investigated the stress relaxation and hysteresis behavior of NR based elastomers vulcanized by sulfur based and peroxide vulcanization system. They also investigated the temperature effect on stress relaxation and hysteresis in their study. The rate of relaxation decreases with an increase in temperature and is attributed to slower nucleation of strain induced crystallites. The decrease in the volume fraction of extendable material as a result of strain induced crystallites has only a small effect on the rate at which the slope of the stress strain curve rises. Hysteresis increases rapidly at strains at which strain induced crystallization becomes possible, but the hysteresis ratio reaches a plateau at higher extensions, supporting the proposal that hysteresis is largely due to the difference between the

degree of crystallinity present on extension and retraction. Also they come up with that an increase in crosslink density limits crystallization and reduce hysteresis.

Masatoshi Tosaka et al [27] studied the crystallization and stress relaxation in highly stretched samples of natural rubber and its synthetic analogue. They made investigations when the stretch ratio was 6. The post stretched relaxation of tensile stress and the development of strain induced crystallization (SIC) were studied by simultaneous measurements of the stress and the diffraction intensities using the synchrotron X-Ray source. They found that in the range of 8s NR crystallized much faster than IR. They proposed that the origin of the superior toughness of NR was from the ability of rapid SIC. To be able to decompose the stress relaxation into its components, namely plastic flow and SIC, they used a formula where the time constants were estimated from the X-Ray study. Then the crystallization time constants were used to decompose the contribution of SIC from the total magnitude of the post stretched relaxation. In the short range of time, the contribution of SIC was found to be dominant. For a tensile strain, SIC plays an important role to reduce the stress. Although this analysis was successful when the stretch ratio was 6, they couldn't find satisfactory results when the ratio was 7.

V.P. Privalko [28] et al worked on the thermo elasticity and stress relaxation behavior of polychloroprene organoclay nano-composites. They used commercial organoclay supplied from Süd-Chemie AG. They prepared the compounds at two stages. In the first step CR was melt compounded with organoclay and the other ingredients. In the second stage vulcanization was carried out by hot stage vacuum press. At the beginning of the study they claimed that with increasing strain the initial spatial aggregates of filler particles spanning the entire sample volume (infinite clusters, IsC); however, the sizes of the latter are believed to be frozen in subsequent stretching/contraction cycles, provided the eventual strains would not exceed the maximum pre-strain. They made stress relaxation tests on the samples which have different amount of organoclay. They saw that experimental data could be best fitted with stretched exponential Kohlrausch equation. The plots of reduced stress vs t for the relaxations $\lambda_f < \lambda_{LIM}$ nicely superpose on the same master curve whereas a similar plot for $\lambda_f = \lambda_{LIM}$ is shifted considerably upwards. As a result they concluded that this result is consistent with the assumption that is made at the beginning of the study.

A.Batra et al [29] studied the stress relaxation of end-linked polydimethylsiloxane elastomer with long pendent chains. They prepared networks by end-linking a mixture of low polydispersity difunctional vinyl terminated PDMS chains and 10 wt % of low polydispersity monofunctional PDMS chains of varying molecular weights using a tetra-functional cross-linker. They found that the stress relaxation moduli under shear can be fitted only in a limited time span by the Chasset-Thirion equation. The exponent m was found to be inversely proportional to the number of entanglements of the pendent chains but a weaker dependence of 0.55.

V.G. Geethamma et al [30] worked on the tensile stress relaxation of short coir fiber reinforced natural rubber composites. They prepared their compounds on a two roll lab scale mills by keeping the nip gap, roll speed and number of passage the same for the different compounds. They examined the effect of strain level, strain rate and short coir fiber on the stress relaxation rate. They showed that the stress decay of unfilled NR samples is independent of the strain. The slope of the stress decay is almost identical for 6% and 60% strain. Rates were -0,037 and -0,027 respectively. However, this rate was higher for high strains, 500% because of the strain induced crystallization behavior of NR. The rate was -0,051 for 500% strain. They showed that as the strain increases strain relaxation increases. When the material is deformed at a higher strain rate, much of the deformation will be reversible and elastic, whereas if it is stressed at a lower strain rate, the individual molecules get time to slip past one another, these results in irreversible, plastic deformation. Hence, one expects to obtain a lower relaxation rate at a higher strain rate and vice versa. Lastly, they showed that the orientation of the coir in the matrix has a effect on the stress relaxation rate.

A.R.R Menon [31] studied the stress relaxation characteristics of natural rubber modified with phosphorylated cashew nut shell liquid prepolymer (PCNLS). He prepared different samples having different amount of PCNLS. He vulcanized the samples with a conventional press at 150^0C and prepared the samples in dumbbell shapes. He conducted the tests in universal tensile machine with different strain rates and strain levels. Strain levels were changing from 50 to 150% and strain rates were 0.0208, 0.1042, 0.2083 s^{-1}. He found that modification of natural rubber with 10-15 phr of PCNSL results in improved tensile properties along with a lower degree of stress relaxation (at higher strain rates and strain levels) compared to unmodified sample. The increase in dosage of PCNSL to 20 phr resulted in a significant increase in the extent and rate of stress relaxation. He also found that at strain

levels ranging from 50 to 120 % and strain rates ranging from 0.0208 to 0.2083 s^{-1}, the stress relaxation characteristics of unmodified and PCNSL modified NR vulcanizates are independent of each other.

L. Zanzotto and J. Stastna [32] studied the dynamic master curves from the stretched exponential relaxation modulus. They worked with the regular pavement asphalt and modified asphalt with SBR. They indicated that the linear behavior of polymer asphalt blends can be described by the general viscoelastic constitutive equation. Asphalt is a thermo rheologically simple material. Thus, one can obtain master curves of various material functions by using the time temperature superposition principle. In this study, they studied the G' and G" of the asphalt and modified asphalt. For the shift factors they used WLF equation. Assuming the relaxation function G(s), has the form of stretched exponential

$$G(s) = C \exp[-(s/\lambda)^{\beta}] \qquad (2.6)$$

where C, λ, β are constants. They derived the storage and loss modulus constitutive equations for the viscoelastic materials. They compared the experimental results with the model. However, they mentioned that it seems impossible to cover a wide frequency interval with one stretched exponential. Therefore, they used different stretched exponential functions for different frequency ranges.

Tarek Madkour [33] investigated the step-strain stress relaxation of carbon black loaded natural rubber vulcanizates. He subjected the samples to a very rapid strain and fixed its length at the deformed state. He investigated the relaxation at different carbon black loadings and at different temperatures. He concluded as the temperature increases, the relaxation times of the polymer composites decrease. Nevertheless, the higher the carbon black content, the slower the relaxation process and the greater the relaxation times will be. The activation energy is independent of the temperature of the stress relaxation experiments, as the temperature affects only the rate of attainment of equilibrium through the increase in the thermal motion of the chains. Increasing the temperature, however, had a lesser effect on decreasing the overall stress values at high carbon black concentrations indicating that thermal motion at these concentrations is less sensitive to the increase in temperature. The increase in the activation energy as a function of the increase in the carbon black

concentration is due to the extra temporary bonds formed between the polymer molecules and the surface active carbon black.

Osman et al [34] worked on the stress relaxation in carbon black loaded butyl rubber. They thermally aged the samples after vulcanization at 90 and 35 days to attain reasonable stability and reproducibility of measured quantities. They worked in compression mode rather than extension mode. They investigated different loadings of carbon blacks under different strain ratios. They concluded that the elastic constant E increases with increasing HAF concentrations in butyl rubber according to the relation

$$E=E_o(1+0.67fc+1.62f^2c^2) \qquad (2.7)$$

with f=6.5. The relaxation time that is calculated from the stress relaxation relation depends on HAF concentration.

G.R. Cotten et al [35] worked on stress relaxation in rubbers containing reinforced fillers. They used BR type rubbers in their study. They prepared their compounds by using lab scale two roll mills. They vulcanized the sheets at 145^0 C and 30 minutes. They made relaxation tests in tension mode if it is cross-linked, compression mode if it is uncross-linked i.e. raw rubber. They found an empirical relation for relaxation as the following;

$$f_t = f_{1.0}\, t^{-n} \qquad (2.8)$$

where $f_{1.0}$ is force after 1 min of relaxation, n is the relaxation rate of the material and t is the time in minutes. They concluded that in both cured and raw butadiene rubbers, stress relaxation was found to be a viscous controlled process. In raw rubbers, reinforcing carbon blacks decrease the rate of relaxation, while in cured rubbers the effect of carbon black is very small. However, in swollen cured rubbers, the rate of relaxation increases with increasing carbon black loadings, indicating a slippage and/or breakage of some carbon black polymer attachments.

Franklin Chang [36] made an investigation on stress relaxation and hysteresis at various strain rates. He used polyisobutylene sheets in 2 mm thick. All specimens were conditioned at 23 ^{0}C and 50% relative humidity for three days. He made all the calculations

based on the Maxwell model and Boltzman superposition principle. He indicated that any one of the three types of stress namely extension, relaxation and hysteresis stresses can be calculated from the other two. However, the time increment in each operation is limited by the value of t_0 which is usually not very large. Although the technique can be applied advantageously for a short range of time, it might be very tedious for the purpose of obtaining a curve of wide range of time. Also, the investigation shows a convenient method to determine hysteresis loss directly from the extension stress time curve. Also he claimed that the relaxation modulus curve determined at various strain rates is essentially the same unique and characteristic curve for each viscoelastic material.

Thor L. Smith [37] worked on the large deformation tensile properties of elastomers. He mainly concentrated on the temperature dependence of C1 and C2 in Mooney-Rivlin equation. In this study he used unfilled butyl and silicone vulcanizates and six hydrofluorocarbon vulcanizates. He derived the C1 and C2 values in Mooney-Rivlin equation from 1 min. isochronal data. He carried out the tests in the temperature range of -20 to 150 ^{0}C for the butyl vulcanizates and -45 to 200 ^{0}C for the silicone vulcanizates. He concluded that C1 increases with temperature at a rate which is in reasonable agreement with published data from the force temperature measurements. Because C2 is sensibly temperature independent over these extended temperature ranges, it was concluded that C2 is a finite quantity under equilibrium conditions. He tested the hydrocarbon vulcanizates between temperature range of -5 to 230 ^{0}C. He concluded that for every sample vulcanizates between 25 and 230 ^{0}C, C1 273/T is temperature independent, but it increases with decreasing temperature below 25 ^{0}C. Except at the lowest temperature, C2 273/T decreases with increasing temperature, the rate of decrease becoming progressively less with an increase in cross-link density.

MacKenzei et al [38] made stress relaxation tests on NR, BR and SBR based rubber containing different loadings of carbon black. They also used unfilled vulcanized rubbers to be able to make comparisons. They plotted σ/σ_0 against log t. The slopes vary little with strain for the NR vulcanizates, but for the BR and SBR, there is some decrease in slope with increase in strain, with the slope leveling off at high strain. For the black loaded NR vulcanized, they obtained two straight lines rather than one as in the gum vulcanizates. The first line of greater slope applying for times less than 1 min. and the second for the greater times. They have also stated that increase in the strain reduces the initial slope, but has little or no effect upon the latter slope. They stated that there are two distinct relaxation processes. For

the longer time process the data well represented by a power law in the time. However, for the short time it is not so precise. Therefore used the double power law for the whole time period, $\sigma(t) = a_1 t^{-n_1} + a_2 t^{-n_2}$ which has 4 adjustable parameters.

Bartenev et al [39] divided the stress relaxation into three processes for the unfilled rubbers and into five processes for the black filled rubbers. Process 1 is due to the orientation and displacement of free segments of chain molecules taking place very rapidly with relaxation times of 10^{-4}-10^{-6}s. Process 2 is due to the regrouping of super molecular structural element with relaxation times within the range of 10^{2}-10^{4}s. This process is responsible for viscous flow in linear polymers. Process 3 is due to the regrouping of the chemical cross-links and chemical bonds in chains both during chemical reactions under the action of stress with relaxation times of 10^{7}-10^{9}s. For the filled elastomers there are two additional processes due to the rupture from filler particles of rubber macromolecules. This process can be given by the formula $\sigma(t) = \varepsilon_0 \sum_{i=1}^{n} E_i e^{-t/\tau}$ where ε_0 is given deformation, E_i is coefficient, τ_i is the relaxation time. For five different processes n= 5 is used. Except τ_5 the relaxation times are independent of deformation in the region of small elongation.

In this review Guth et al. [40] mentioned about the Einstein's viscosity theory of a suspension. Einstein viscosity theory has the following form;

$$\eta = \eta_0 (1 - 2.5\upsilon / V) \tag{2.9}$$

where η is the viscosity of the solvent, η_0 is the viscosity of the suspension, υ is the total volume of the suspended particles V is the volume of the suspension. However this equation holds only for small concentrations. For higher concentrations one must take into account the mutual disturbance caused by a pair of particles of a laminar stream. This has been done by H.A. Lorentz and the equation became

$$\eta = \eta_0 (1 - 2.5\upsilon / V - 14.1\upsilon^2 / V^2) \tag{2.10}$$

This equation is applicable to all solutions of high molecular weight substances with spherical shape, such as rubber latex solutions, protein solutions and the changing of the viscosity of

lubricating oils by the addition of small quantities of higher molecular compounds. The equation was verified experimentally in the case of suspended glass spheres.

Guth [41] worked on the theory of reinforcement. He stated that the well known Einstein's viscosity equation has the following form;

$$\eta^* = \eta[1 + 2.5c] \tag{2.11}$$

where η^* and η are the viscosity of the emulsion and solvent and c is the volume concentration. Einstein's theory of viscosity gives a pattern for similar theories of other physical properties of suspensions of colloidal particles in a continuous medium, whether this medium be fluid or solid. For instance, properties which may be discussed in this way include Young's modulus, thermal conductivity, and dielectric constant. He subdivided the carbon black- polymer mixtures to the three categories. First one is the one where loadings are till 10 %. In this category carbon blacks are well separated from each other. In the second one the loadings are up to 30 % where a network is formed between the carbon black particles. In the last category where the loadings are greater than 30 %, carbon blacks are tightly stacked. Lorentz modified the Einstein's theory for the higher concentrations and it was applied to elastic properties first by Rehner. The computation of the change in the elastic constants of rubber by the embedded black spheres is entirely analogous to the procedure in the theory of viscosity. If a rubber black suspension is stretched, the suspended particles perturb the stresses, and strains set up in the body. This perturbation leads to an increase in the elastic energy. This in turn gives an increase in the elastic constants i.e. a stiffening of the stock. Therefore, Young's modulus can be given by the following formula;

$$E^* = E[1 + 2.5c + 14.1c^2] \tag{2.12}$$

If the concentration increases above 10 percent, the stiffness of the stocks increases much more rapidly than equation would predict given above. This is the formation of chains by the spheres. One can study this accelerated stiffening more quantitatively by considering rod like filler particles embedded in a continuous matrix. For this model one obtains as an analog of equation above;

$$E^* = E\left[1 + 0.67 f.c + 1.62 f^2.c^2\right] \qquad (2.13)$$

Here f is the shape factor (=length/breadth) of the rod, and he has assumed f>>1. This equation clearly exhibits the rapid increase of modulus with increasing concentration.

H.M. Smallwood [42] worked on the reinforcement of rubber. He used natural rubber based compound and used many fillers to correlate them with Einstein's viscosity relation. He used carbon blacks, whitening from different sources and zinc oxide again from different suppliers and clay. He compared the experimental results with the theoretical ones. There are deviations in carbon black loaded ones interpreted as being the flocculation of the carbon black in the matrix. Compounds filled with clays have higher modulus values than model predicted. It was interpreted as being the acicular shape of the clay particles. Whitening gives good correlation with the model. Lastly, zinc oxide filled compounds had higher modulus values than model. It couldn't be explained clearly in the paper.

A.I. Medalia [43] investigated the immobilization of rubber occluded within carbon black aggregates. He proposed that in a carbon black-rubber system the rubber which fills the void space within each aggregate is occluded and immobilized and thus acts as part of the filler rather than as part of the deformable matrix. The amount of occluded rubber can be calculated directly from the DBP absorption value of the carbon black. However he made assumptions regarding the distribution of void space within and between the aggregates. It was suggested that at the end point of oil absorption test the packing of the aggregates was intermediate between "close" and "random" packing so that the void space between the aggregates amounted to 31.5% of the total volume of the system. Secondly, at the DBP endpoint the system contains around 15% air. Based on these assumptions he correlated the DBP absorption of the carbon black with occluded rubber. He also introduced the effectiveness of this occluded rubber and this was found as 0.5.

K.L. Ngai and C.M. Roland [44] worked on the junction dynamics and proposed Coupling Model. The coupling model is an attempt to provide a unifying picture of the constrained dynamics of relaxation phenomena in a dense phase. They claimed that motion of any moiety in a dense packed system is governed by constraints originating from intra-molecular and intermolecular interactions with other groups. At short times each moiety

relaxes independently, the dynamic constraints not having built up to an extent sufficient to impede the motion. In this short time regime, the relaxation rate can be expressed in terms of the transitions of independent moieties. The correlation function describing the independent relaxation in this short time regime has the exponential form. However, from general physical principles, there exits a time scale after which the average relaxation rate of the moieties will be slowed down by the dynamic constraints. As a consequence, the normalized correlation function that describes the relaxation of a macroscopic variable will have the stretched exponential form;

$$C_c(t) = \exp\left[-\left(t/\tau^*\right)^{1-n}\right], \quad t>t_c \tag{2.14}$$

where

$$\tau^* = \left[(1-n)t_c^{-n}\tau_0\right]^{1/(1-n)} \tag{2.15}$$

where τ_0 is the inverse of relaxation rate, t is time, t_c is the critical time and n is the exponent. Although this model gives good results in some viscoelastic properties, a number of anomalies exist without any explanation.

CHAPTER 3

3. EXPERIMENTAL:

In this section, the details of the experimental part will be given. The details of the raw materials used, compounding, vulcanization and stress relaxation tests will be explained. The details of the equipments used will also be given in this section.

3.1 Materials Used

The raw materials used in this recipe were Natural rubber (polyisoprene), Zinc Oxide, Stearic Acid, CBS (N-cyclohexyl-2-benzothiazole sulphenamide), Carbon black (N330) and Sulfur. All the raw materials were used as received. All the specification values given here have been taken from the analysis reports of the raw materials used. The natural rubber grade was Ribbed Smoked Sheet, RSS1, with a Mooney viscosity of 85 Mooney Units, MU, at 100°C, MW≈350000 and a polydispersity index of 2.5, supplied from Eversharp Rubber Industries, Jalan, Singkang, Jementah, Johor. Zinc oxide, 99,7 % purity with a 550 g/l bulk density was supplied from Metal Oksit (www.metaloksit.com). Stearic acid with an acid value 208,8 mg KOH/g, fatty acid composition 55,2 % C16, 44,2% C18 was supplied from Natoleo (www.natoleo.co.kr). Carbon black was supplied from TUPRAŞ (www.tupras.com.tr) with a DBP absorption of 102 ml/100g, with an iodine adsorption of 83.2 mg/g and with a bulk density of 378 g/l. CBS was supplied from MLPC. Its melting point was 97°C, ash content was 0,3% and specific gravity was 1,27. Sulfur was supplied from MLPC (www.mlpc-intl.com). Its melting point was 115 °C and specific gravity was 2,04.

3.2 Compounding

Compounds were prepared by using a lab scale 1,5 liter Werner & Pfleiderer internal mixer. This internal mixer has standard tangential rotor geometry. The homogenizations were made on the two roll open mills. Rubber was fed into the chamber, masticated for 2 minutes and then Zinc Oxide and Stearic acid were added. The compound was dumped at around 135 °C. It homogenized on the two roll mill for 5 minutes. In the second stage, for the filled elastomers first of all carbon black incorporated and then accelerator and sulfur were added on the two roll mill for different compounds.

3.3 Vulcanization

Vulcanization was carried out in a compression molding with 160 t clamping force. All test sheets were vulcanized at 150°C/ 35min. The test sheet dimensions were 210x300x2 mm^3.Before the test sheets were vulcanized, rheometer curves were checked at 150 °C which is the temperature at which the test sheets were vulcanized later on. The rheometer used is from Alpha Technology, MDR 2000. The rheometer curves showed that the torque values reach a plateau and remained constant from thereon, indicating that there is no reversion. The optimum cure times were obtained between 25-30 minutes depending on the different cross-linking densities in the rheometer curves. To be on the safe side, all sheets were vulcanized at 150°C for 35 minutes knowing that there is no reversion for these recipes.

3.4 Relaxation Tests

Dumbbell shaped test specimens of 2 mm thickness were cut out from the vulcanized sheets with the help of a Zwick sample cutter in accordance with DIN 53 504, S1. Relaxation tests were carried out in a Zwick Roell Z2,5 universal tensile machine (UTM) with a load cell of 2,5 kN. Extension data were acquired at every 10 microns with an accuracy of 1%. The

equipment used testXpert V10.1 version software. Dumbbell shaped test sheets were tested at UTM with a pre-load of 0,2 N that prevented the initial curvature of the free samples. Test sheets were stretched to different extension ratios at a speed of 800 mm/min, and relaxed for 880 sec. for every sample. Data was taken at every 0.02 s. during the test.

CHAPTER 4

4 RESULTS AND DISCUSSION

In this section, experimental and computational results are given and detailed discussions will be made. This section can be divided into two sections. The first section is the networks without carbon black namely unfilled section and the second one is the networks containing carbon black namely filled section. In both sections the details of the theoretical works will be given and then the experimental results and theoretical results will be compared.

4.1 Unfilled Samples

4.1.1 Theory and Model

At equilibrium, a network junction exhibits large-scale fluctuations about its mean position. This is because the pendent chains to the junction exhibit large-scale diffusive motions about their equilibrium configurations. In a tetra-functional phantom network where there are no constraints to suppress junction fluctuations, mean squared fluctuations $\left\langle (\Delta R)^2 \right\rangle$ of a junction are related to the mean-squared end-to-end distance $\left\langle r^2 \right\rangle_0$ of a network chain by [9] $\left\langle (\Delta R)^2 \right\rangle = \frac{3}{8}\left\langle r^2 \right\rangle_0$. For a polyisoprene network with reduced stress, $[f^*] = 0.1 Nmm^{-2}$, the radius of the fluctuation domain for a junction at equilibrium is about 50 Å and there are about 50 cross-links that share this domain. In real networks this sphere is smaller due to

constraints. According to the constrained junction model, [12,45] the mean-squared radius of the domain in which a network junction fluctuates is inversely proportional to the constraint parameter, κ_0. This parameter is defined as the ratio

$$\kappa_0 = \frac{\left\langle \Delta R^2 \right\rangle_0}{\left\langle \Delta s^2 \right\rangle_0} \tag{4.1}$$

where, $\left\langle \Delta R^2 \right\rangle_0$ is the mean-square fluctuation of the junction in the phantom network and $\left\langle \Delta s^2 \right\rangle_0$ is the corresponding value in the real network, in the presence of constraints. The value of κ varies between 0 for highly cross-linked networks and about 10 or 12 for lightly cross-linked networks.

The diffusive motions of junctions have been observed in spin echo experiments [46]. These experiments, carried out on poly(dimethylsiloxane) networks with labeled junctions showed that the junctions move diffusively with characteristic relaxation times of 1-10 ns in a region whose size agrees with the predictions of the constrained junction model. The factors that effect the diffusion times of a junction comes from its steric interactions with the entanglement domain and from the network chains that are covalently attached to it at the ϕ functional junction.

According to the constrained junction model, the entanglement domains transform affinely with macroscopic deformation. In a deformed network at equilibrium, the junctions fluctuate in an affinely transformed domain. Given the sufficiently long time, they can explore all points in this domain, as shown by the spin echo experiments. At short times following a sudden stretch, the junction does not have a chance to explore all points available to it at equilibrium. It explores the small vicinity of its position during the moment of stretch. As the network is allowed to relax, however, the junction diffusively explores larger and larger regions of the constraint domain. Stated in another way, the size $\left\langle (\Delta s)^2 \right\rangle$ of the domain that appears in the definition of the κ parameter, Eq. 4.1, in which the junction can fluctuate is small at short times following the stretch and spreads out as time progresses. Thus, the κ parameter should be a function of time. The time dependent contributions to κ are expected to be large at short times following the sudden stretch and vanish with time as equilibrium is

approached. The process may be followed easily through the time dependence of the $2C_1$ and $2C_2$ parameters where the former reflects the dynamics operating below length scales of $\left[\left(\frac{M_e}{M_c}\right)\left\langle r^2\right\rangle_0\right]^{1/2}$ while the latter reflects the dynamics at length scales of $\left\langle r^2\right\rangle_0$ or larger. Here, M_c is the molecular weight of a network chain, and $\left\langle r^2\right\rangle_0$ is the mean-squared end-to-end distance of the unperturbed network.

Based on the above discussion, we write the force *f(t)* acting on the network at time t as

$$f(t) = f_{ph} + f_{c,eq} + f_c(t) \tag{4.2}$$

where, f_{ph} is the component of force due to the phantom network, and $f_{c,eq}$ and $f_c(t)$ are the equilibrium and non-equilibrium forces due to constraints, respectively.
For uniaxial deformation, [9]

$$f_{ph} = \left(\frac{\xi kT}{L_0}\right)\left(\lambda - \frac{1}{\lambda^2}\right) \tag{4.3}$$

Here, L_0 is the length of sample, and ξ is the cycle rank of the network denoting the number of chains that should be cut in order to reduce the network to a tree. The second term $f_{c,eq}$ in Eq. 4.2 is given by the constrained junction model as

$$f_{c,eq} = f_{ph}\left[\frac{\lambda K(\lambda) - \lambda^{-2}K(\lambda^{-1})}{\lambda - \lambda^{-2}}\right] \tag{4.4}$$

where,

$$K(\lambda) = B\left[\frac{\dot{B}}{B+1} + \kappa^{-1}\frac{\lambda^2\dot{B}+B}{B+\kappa_0\lambda^{-2}}\right] \tag{4.5}$$

$$B = \kappa_0{}^2 \frac{\lambda^2 - 1}{\left(\lambda^2 + \kappa_0\right)^2} \tag{4.6}$$

$$\dot{B} = B\left[\frac{1}{\lambda^2 - 1} - \frac{2}{\lambda^2 + \kappa_0}\right] \tag{4.7}$$

The fundamental assumption of the theory of irreversible thermodynamics is that the functional dependence of local entropy on the local extensive parameters is identical to the dependence in equilibrium [47]. This assumption allows us to extend the equilibrium constraint theory to the time domain, according to which the term $f_c(t)$ in Eq. 4.2 now reads as

$$f_c(t) = f_{ph}\left[\frac{\lambda K(\lambda, t) - \lambda^{-2} K(\lambda^{-1}, t)}{\lambda - \lambda^{-2}}\right] \tag{4.8}$$

where the time dependence is introduced to the K function as

$$K(\lambda, t) = B(t)\left[\frac{\dot{B}(t)}{B(t) + 1} + \kappa(t)^{-1} \frac{\lambda^2 \dot{B}(t) + B(t)}{B(t) + \kappa(t)\lambda^{-2}}\right] \tag{4.9}$$

with

$$B(t) = \kappa(t)^2 \frac{\lambda^2 - 1}{\left(\lambda^2 + \kappa(t)\right)^2} \tag{4.10}$$

$$\dot{B}(t) = B(t)\left[\frac{1}{\lambda^2 - 1} - \frac{2}{\lambda^2 + \kappa(t)}\right] \tag{4.11}$$

The parameter $\kappa(t)$ now becomes the only additional parameter to describe the relaxation behavior of the networks. The junction performs Brownian motion under the joint action of the pendent chains and the constraint domain. We assume that the pendent chains impose quickly varying forces on the junction relative to the response of the constraint

domain. The latter provides the friction force. The motion of the junction may then be studied by the Langevin equation.

In real networks, there are several relaxation pathways of different time scales that contribute to the time dependent κ parameter. In general these are such that the relaxation through one pathway depends on the prior relaxation through another pathway. In order to introduce such dependencies, the functional form of $\kappa(t)$ should show more diffuse dependence on time. Two such possible forms are

$$\kappa(t) = \kappa_0 \exp\left[-\left(\frac{t}{\tau}\right)^{\beta}\right] \qquad \kappa(t) = A\left(\frac{t}{\tau}\right)^{-m} \tag{4.12}$$

where, τ is the characteristic time of relaxation of constraint effects, β is the exponent, m is the power, and κ_0 and A are the front factors. The expression on the left in Eq. 4.12 is the stretched exponent form, and the one on the right is a power form, originally used by Chasset and Thirion [48] to describe the long time relaxation of natural rubber networks. The two functions exhibit significant differences, both at short and long times. The power relation diverges as time goes to zero. It shows much faster decay than the stretched exponent at short times, and much slower decay at long times. Comparison with experimental data, as will be discussed in more detail below, showed that the power relation does not represent relaxation satisfactorily whereas the stretched exponent shows almost perfect agreement with data. We therefore adopt the stretched exponent form.. The stretch exponent β, indicating the multiexponential behavior of relaxation, is different than unity as will be shown in the experimental validation of the theory below.

The theoretical model presented in this section is valid only at long times at which the time dependence of the $2C_1(t)$ term has vanished in Mooney Rivlin equation as given in Introduction section. There are excellent theories of rubber viscoelasticity that describe the short time behavior in which the transient entanglement network contribution is significant [49]. In the following section, we present an experimental validation of the Dynamic Constrained Junction Model.

4.1.2. Experimental Validation

The sample details used in this section is presented in Table 4.1

Table 4.1 Sample notation for unfilled samples

Sample Notation	Sulphur amount, phr
S01	0,75
S02	1,0
S03	1,25

In Figure 4.1-4.3, the isochronous plots for networks for different cross-link densities were presented. The ordinates denote the reduced stress $[f^*]$ and the abscissas are the reciprocal extension ratios. The points show the results of experiments. The shortest time of observation is one second. The longest time of 880 seconds recorded in the experiments did not correspond to full equilibrium, but sufficiently close to it for all of the samples. The curves are obtained from the theory presented in method and theory section.. They are obtained for each figure as follows: First a value for κ_0, and $[f_{ph}^*]$ is assumed. We also assumed the stretched exponential form for the function $\kappa(t)$. For a given value of τ and β the calculated $[f^*]$ values are compared with $[f^*]$ values obtained from experiments. The calculations are repeated and the (τ,β) pair that gives the best agreement is accepted. The same procedure is repeated for each figure. The relaxation time of 40 s that gives the best agreement of theory with experiment is the same for all four samples.

The parameters for Dynamic Constrained Junction Model for unfilled samples were presented in Table 4.2

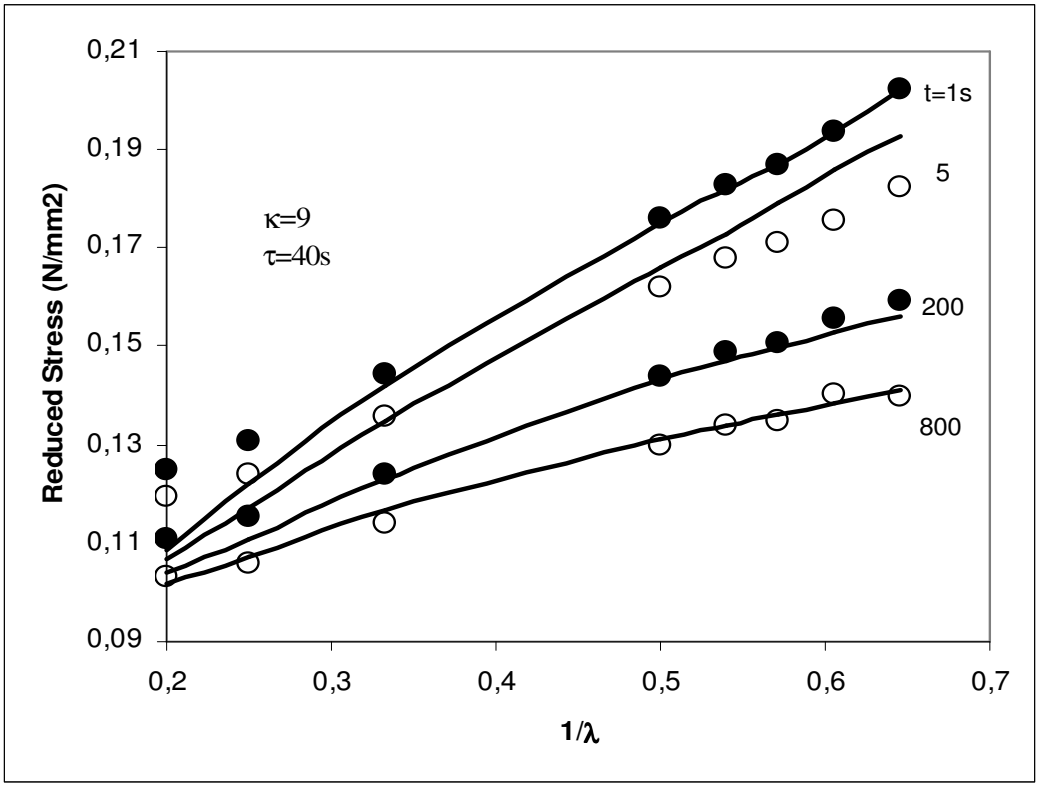

Figure 4.1 Isochronous plots of Sample S01 and comparison with Dynamic Constrained Junction results.

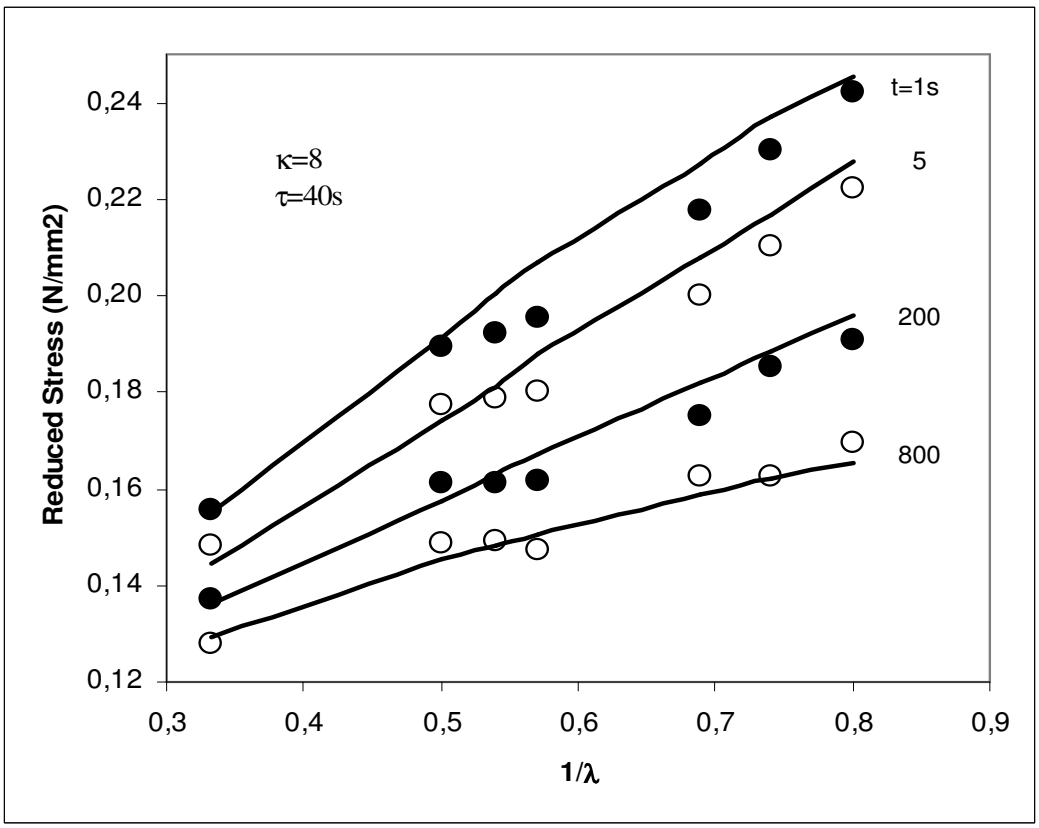

Figure 4.2 Isochronous plots of Sample S02 and comparison with Dynamic Constrained Junction results.

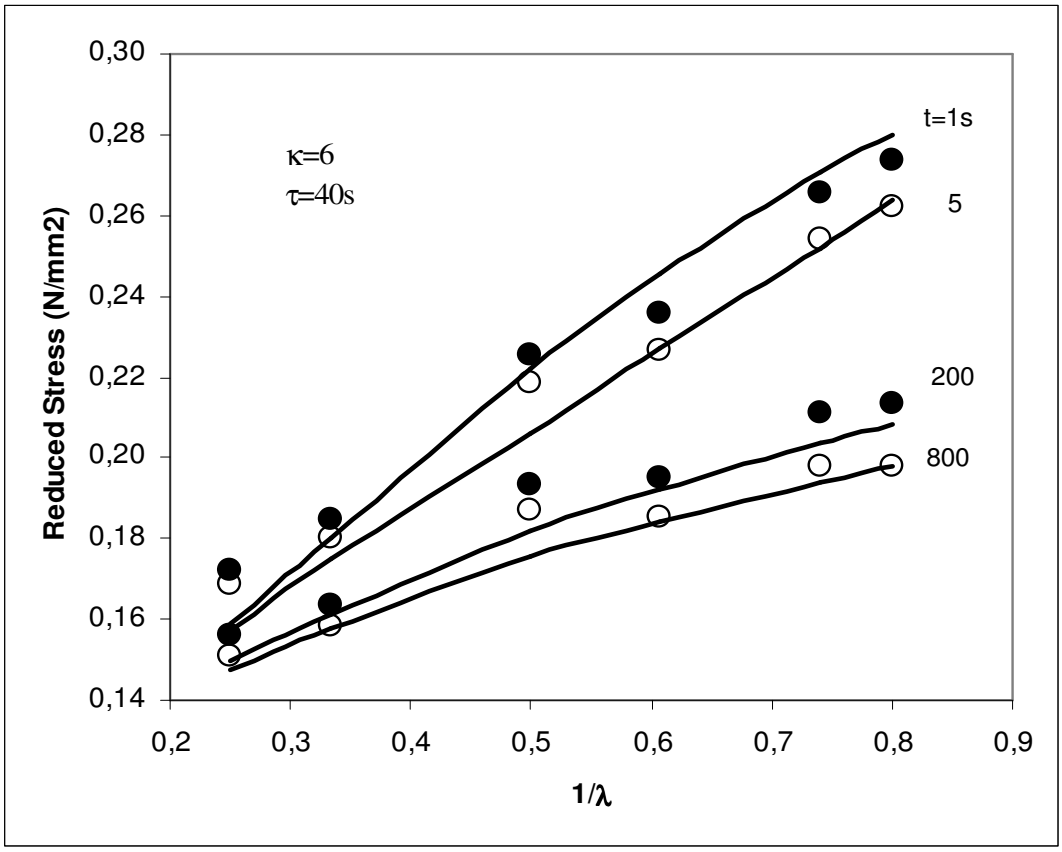

Figure 4.3 Isochronous plots of Sample S03 and comparison with Dynamic Constrained Junction results.

Table 4.2 The parameters for Dynamic Constrained Junctions model for unfilled samples

Sample Notation	f_{ph}(Mpa)	κ_0	τ (Relaxation time,s)	β (Exponent)
S01	0.092	9	40	0,4
S02	0.104	8	40	0,4
S03	0.132	6	40	0,4

In Figures 4.4-4.6, the dependence of stress on time is presented for the samples

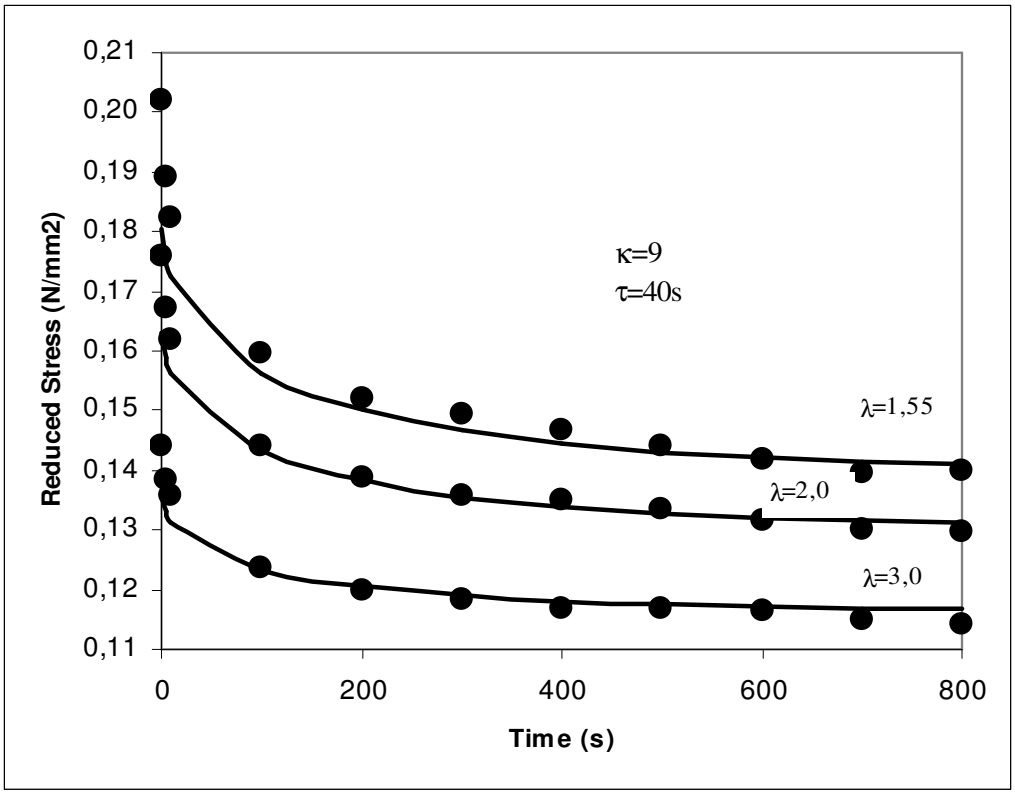

Figure 4.4 Dependence of stress on time for S01

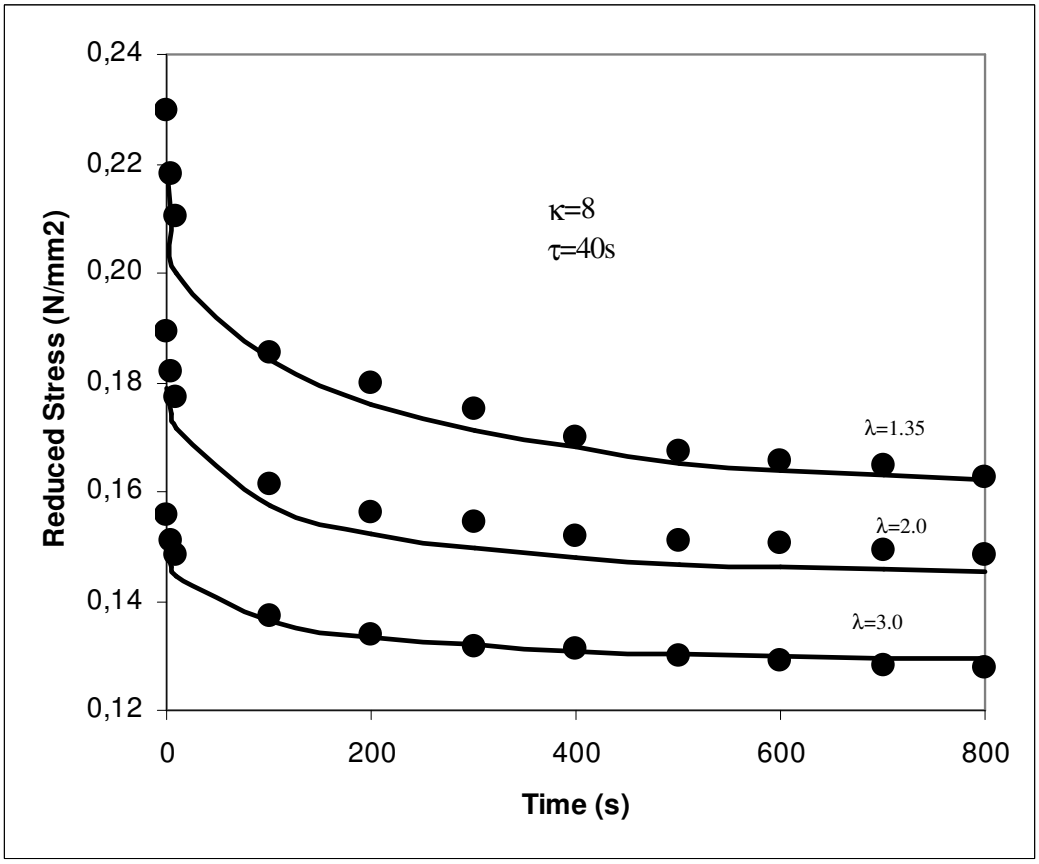

Figure 4.5 Dependence of stress on time for S02

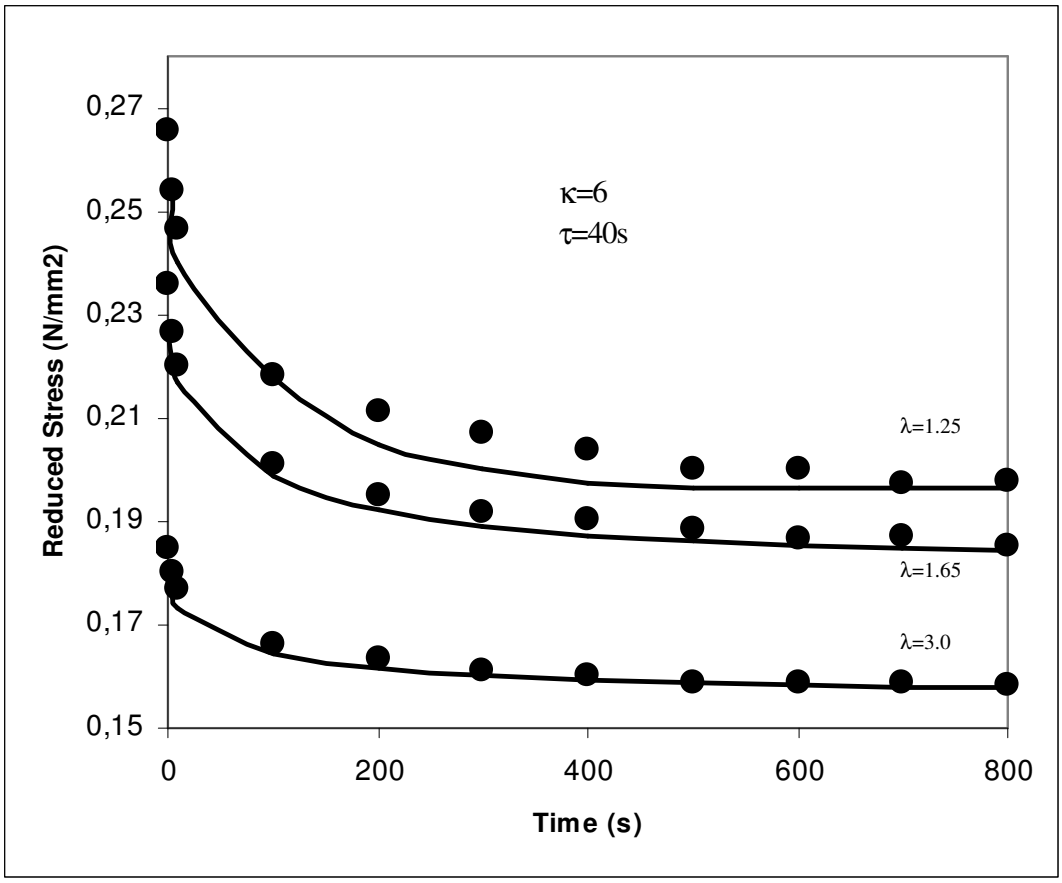

Figure 4.6 Dependence of stress on time for S03

In this section, we extended the equilibrium constrained junction model to stress relaxation in uniaxial extension. In line with the fundamental assumption of irreversible thermodynamics, we took the functional dependence of the out of equilibrium stress on deformation same as given by the equilibrium theory. Results based on this simplification are in excellent agreement with experiment. Relaxation is described by a single parameter, $\kappa(t)$ which leads to experimental data only if it is of the stretched exponent form. This form, which is known as the Williams-Watts-Kohlrauch form in phenomenological theories, may be taken as an indication of serial cooperativity where different pathways of relaxation exist in which one relaxation step depends on the occurrence of another. Stated in another way, relaxation goes through hierarchically constrained steps: Sudden stretching of the network causes an affine-like deformation of chains. Chains deformed in this manner do not relax all at once. A group of chains relax first, this induces the relaxation of others, through network connectivity. Thus, according to this interpretation, relaxation propagates from one junction to its topological neighbors in a serial fashion. We would like to indicate that this interpretation, although plausible, is one of several other possible relaxation pathways. This type of

hierarchical relaxation was introduced by Palmer et al., [49] and since then has been adopted for relaxation in a diverse field of materials.

4.2.Filled Samples

4.2.1 Theory and Model

Filers are incorporated into rubbers to increase the strength of vulcanizates. Thus it is hardly surprising that relatively few applications of elastomers use the polymer in the unfilled state. Reinforcement signifies primarily an increase in ultimate properties such as tear and tensile strength and abrasion resistance and is most pronounced with non-crystallizing rubbers. Fillers also increase the modulus of elasticity and are often added for this purpose [7]. The Einstein's theory of viscosity [40,42]which relates the viscosity of the suspension to the viscosity of the solvent with the volume fraction of the suspended particles is given as

$$\eta^* = \eta(1 + 2.5\phi) \tag{4.13}$$

where η^* is the viscosity of the suspension η is the viscosity of the solvent and ϕ is the volume fraction of the suspended particles. Guth and Gold [41] later extended this equation to the higher concentrations taking inter-particular disturbances into account.

$$\eta^* = \eta(1 + 2.5\phi + 14.1\phi^2) \tag{4.14}$$

where the notations are the same as given above. Einstein's theory of viscosity gives a pattern for similar theories of other physical properties of suspensions of colloidal particles in a continuous medium, whether this medium be fluid or solid [41]. For instance, properties which may be discussed in this way include Young's modulus, thermal conductivity and dielectric constant. Medalia [43] added 'occluded rubber' volume to the actual carbon black filler volume to obtain the 'effective' volume of the rigid phase. 'Occluded rubber' was defined as the rubber part of the elastomeric matrix which penetrated the void space of the individual carbon aggregates, partially shielding it from the deformation. He obtained the

'occluded volume of the rubber' by using the DBP absorption value of the filler used. He used the effective volume in Guth and Gold equation instead of the volume fraction of the filler itself.

The sample details used in this section is presented in Table 4.3

Table 4.3 Sample notation for the filled samples

Sample notation	Effective filler volume fraction, ϕ	Sulphur amount, phr
S11	0.0397	0.75
S12	0.0397	1.00
S13	0.0397	1.25
S21	0.0799	0.75
S22	0.0799	1.00
S23	0.0799	1.25
S31	0.1129	0.75
S32	0.1129	1.00
S33	0.1129	1.25

As it is given in unfilled section, Dynamic Constrained Junction Model captures the isochronous Mooney plots and stress relaxations of the vulcanizates successfully for the unfilled and different cross-link density samples. In this section, this theory is extended for the filled and the different cross-link density amorphous polymeric networks as well.

In the Dynamic Constrained Junction Model force acting on the network is given as in Eq 4.2. where, f_{ph} is the component of the force due to the phantom network, and $f_{c,eq}$ and $f_c(t)$ are the equilibrium and non-equilibrium forces due to the constraints, respectively. In this section, the basic assumption is that the force due to the phantom network, and the equilibrium and non-equilibrium forces due to the constraints follow the Guth and Gold equation when fillers are added into the matrix and these three terms can be written as follows;

$$f_{ph} = \left(f_{ph}\right)_0 \left(1 + 2.5\phi + 14.1\phi^2\right) \tag{4.15}$$

$$f_{c,eq} = \left(f_{c,eq}\right)_0 \left(1 + 2.5\phi + 14.1\phi^2\right) \tag{4.16}$$

$$f_c(t) = \left(f_c(t)\right)_0 \left(1 + 2.5\phi + 14.1\phi^2\right) \tag{4.17}$$

where subscript 0 describes the unfilled amorphous network, ϕ is the effective volume fraction which includes the occluded rubber as mentioned in the introduction section. When we rearrange Eq 4.2 by multiplying and dividing by f_{ph} then we obtain:

$$f(t) = \left(f_{ph}\right)\left[1 + \frac{\left(f_{c,eq}\right)}{\left(f_{ph}\right)} + \frac{\left(f_c(t)\right)}{\left(f_{ph}\right)}\right] \tag{4.18}$$

in this equation the second and the third terms in the bracket are independent of ϕ and only the third term is time dependent. Additionally, only the first f_{ph} term of the right hand side of the equality is ϕ dependent.

4.2.2. Experimental Validation

The curves are obtained from the theory presented in unfilled section with the exception that $f(t)$ is calculated by using Eq.4.18 given in this section. The fitting parameters of τ, β, $\left(f_{ph}\right)_0$ were calculated for the unfilled different cross-link density samples in unfilled section and used in this section as they are. These parameters can be seen in Table 4.2 as well. Only fitting parameter in this section is the κ_0 for the filled samples and presented on each graph. κ_0 values are given in Table 4.4

Table 4.4 The κ_0 values for Dynamic Constrained Junction model for filled samples

Sample Notation	κ_0
S11	10,5
S12	11,5
S13	9
S21	5,5
S22	10,5
S23	3,5
S31	9,5
S32	11
S33	8

We present isochronous Mooney plots for filled samples in Fig. 4.7 -4.15

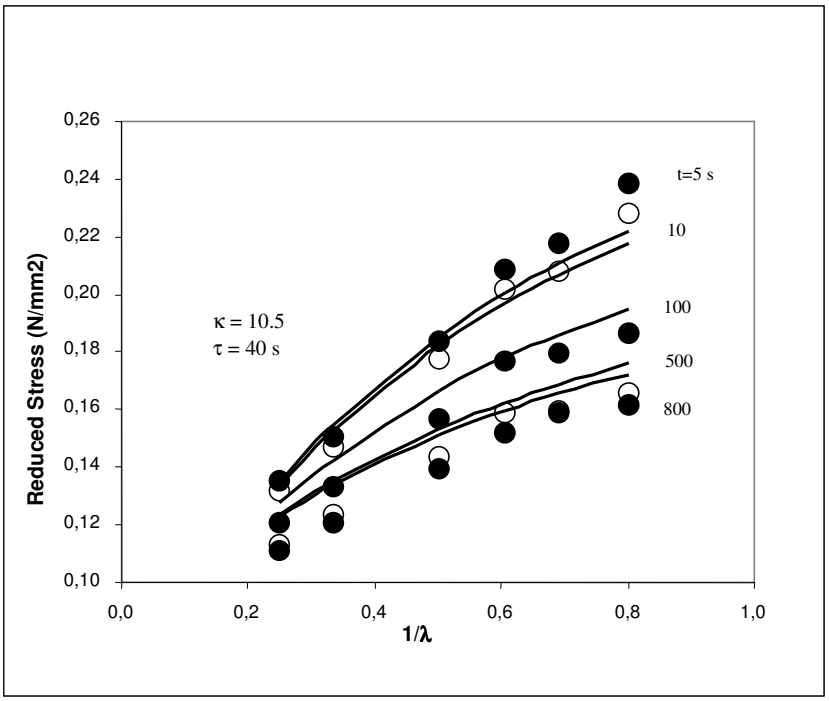

Figure 4.7 Isochronous plots of Sample S11 and comparison with the Dynamic Constrained Junction Model results.

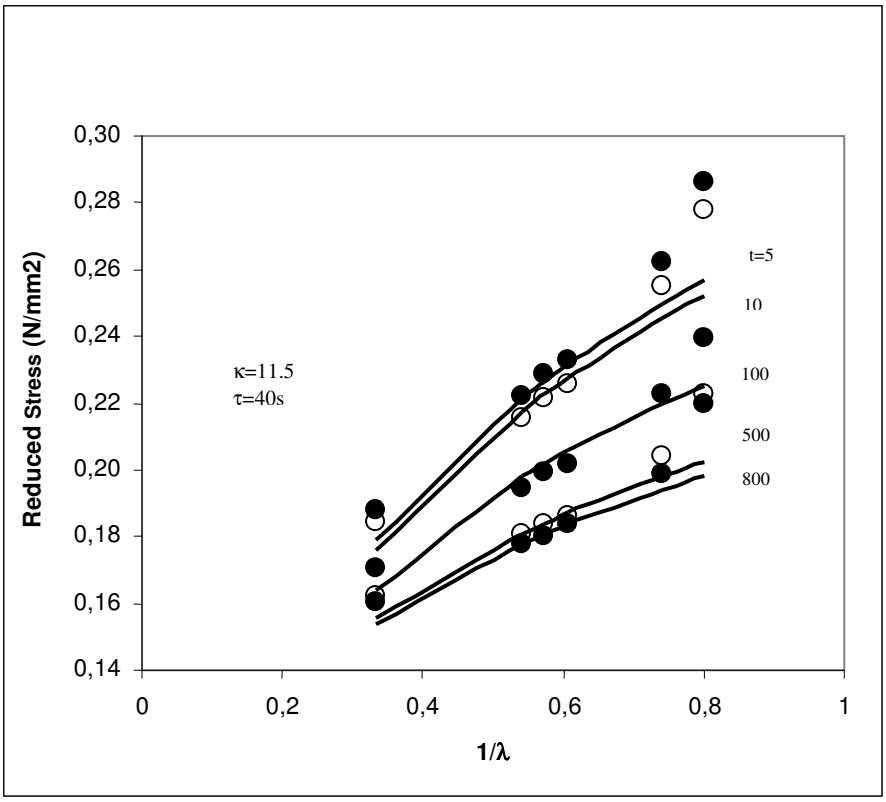

Figure 4.8 Isochronous plots of Sample S12 and comparison with the Dynamic Constrained Junction Model results.

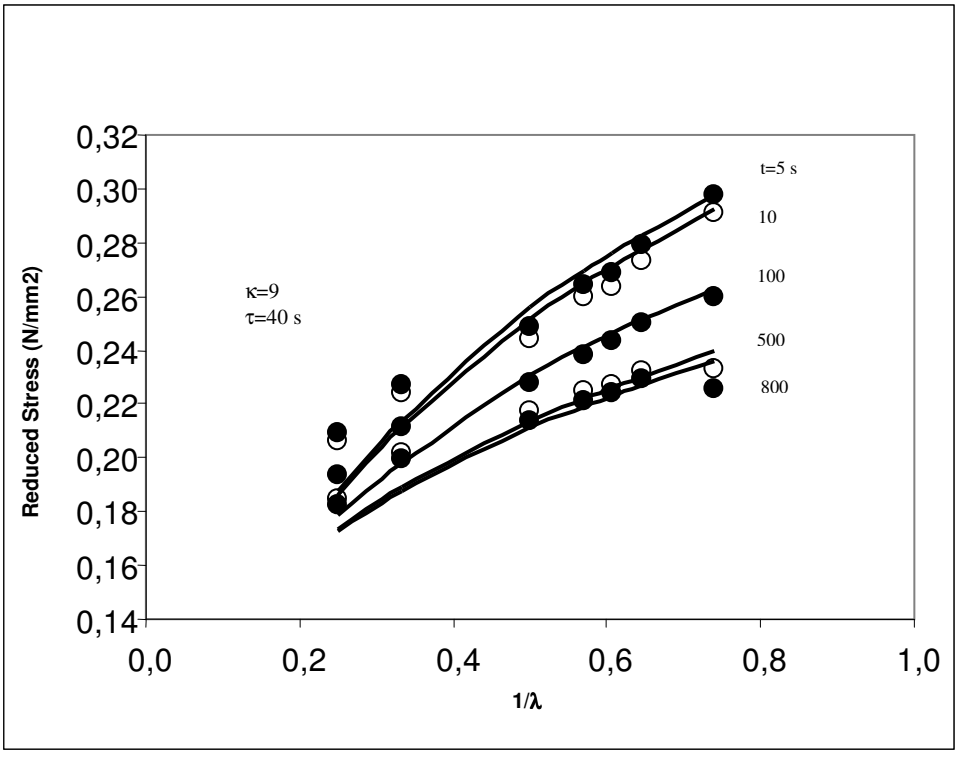

Figure 4.9 Isochronous plots of Sample S13 and comparison with the Dynamic Constrained Junction Model and results.

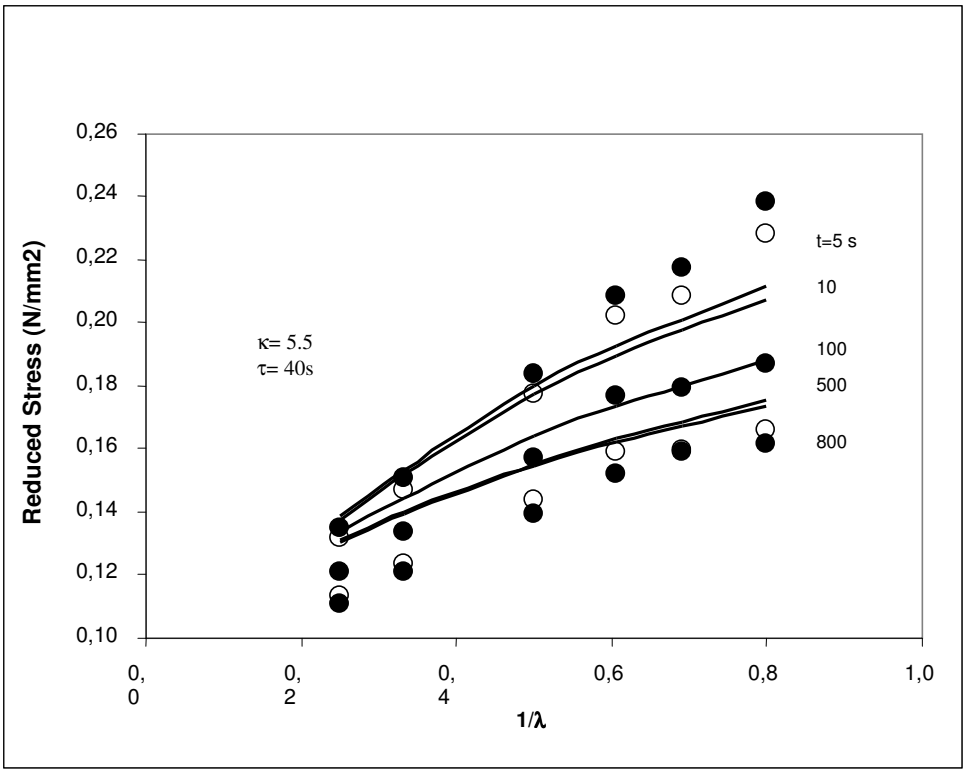

Figure 4.10 Isochronous plots of Sample S21 and comparison with the Dynamic Constrained Junction Model and results.

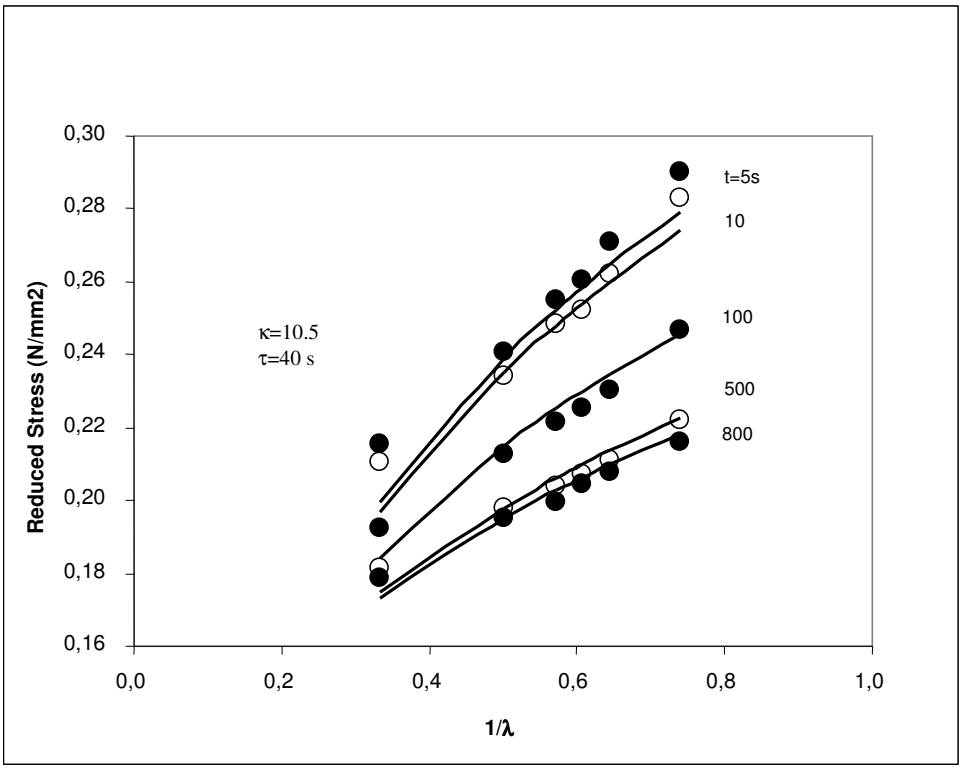

Figure 4.11 Isochronous plots of Sample S22 and comparison with the Dynamic Constrained Junction Model and results.

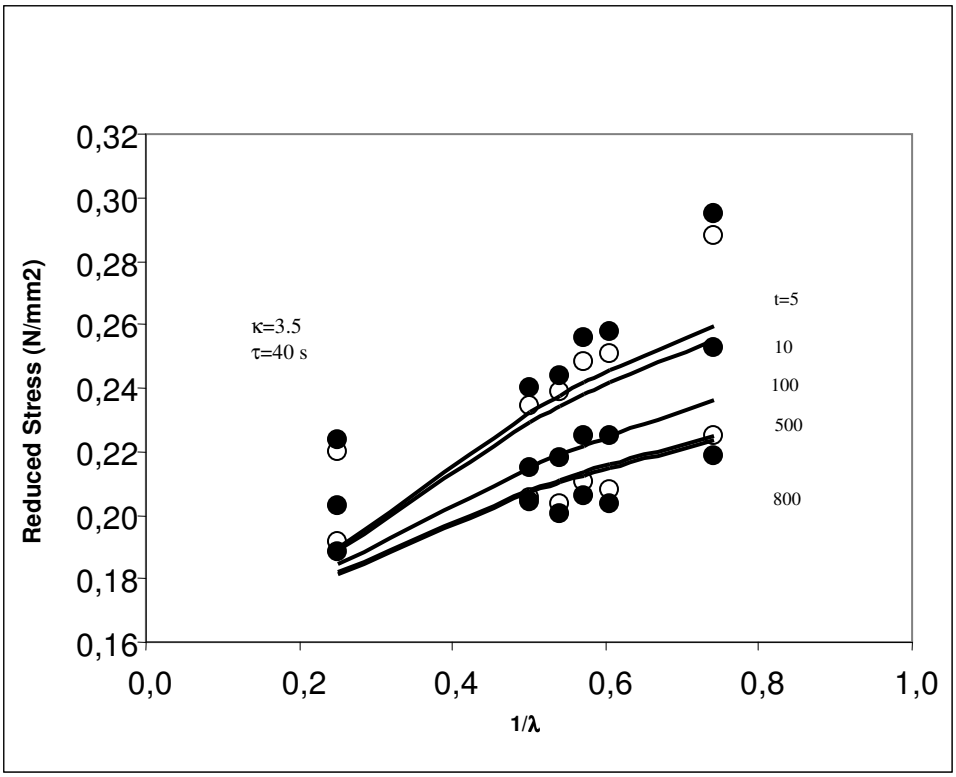

Figure 4.12 Isochronous plots of Sample S23 and comparison with the Dynamic Constrained Junction Model and results.

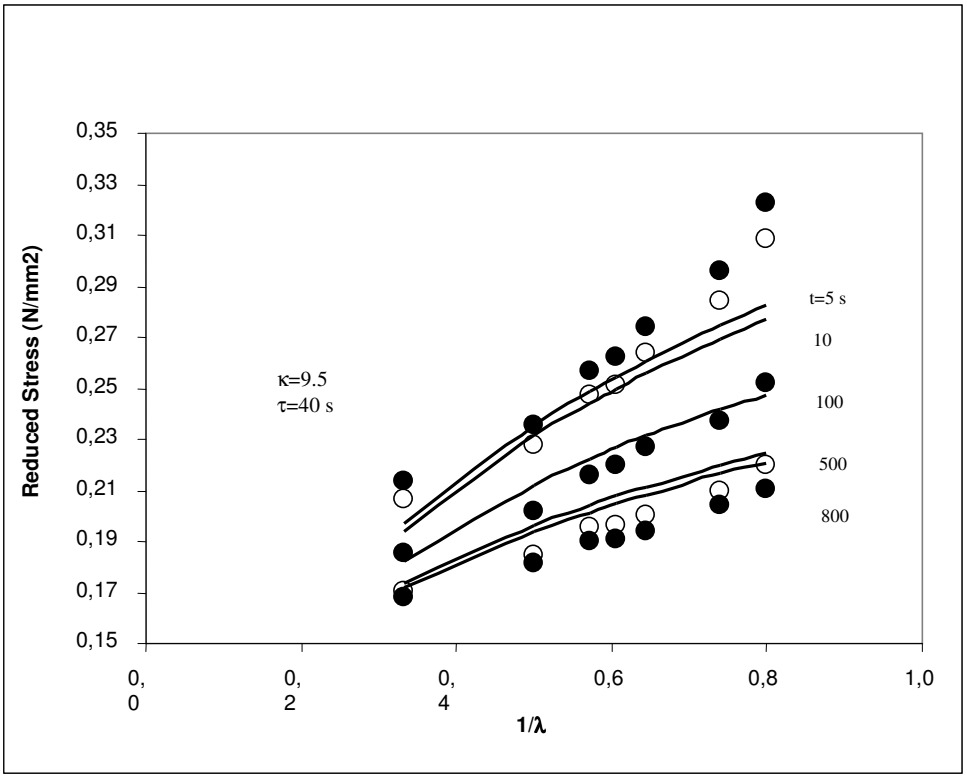

Figure 4.13 Isochronous plots of Sample S31 and comparison with the Dynamic Constrained Junction Model and results.

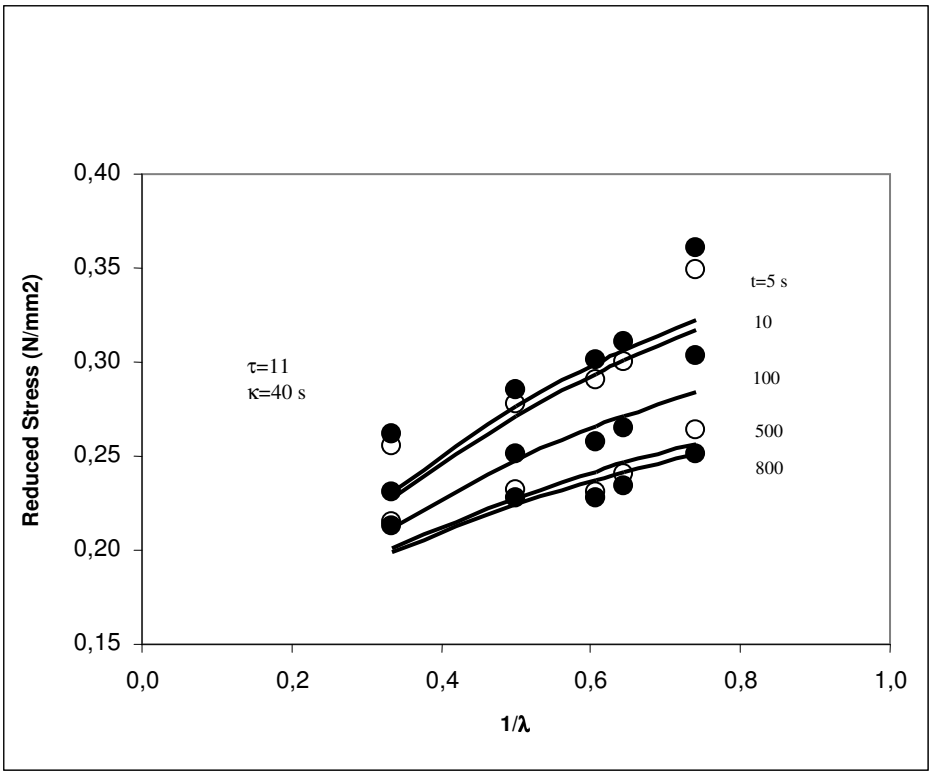

Fig.4.14 Isochronous plots of Sample S32 and comparison with the Dynamic Constrained Junction Model and results.

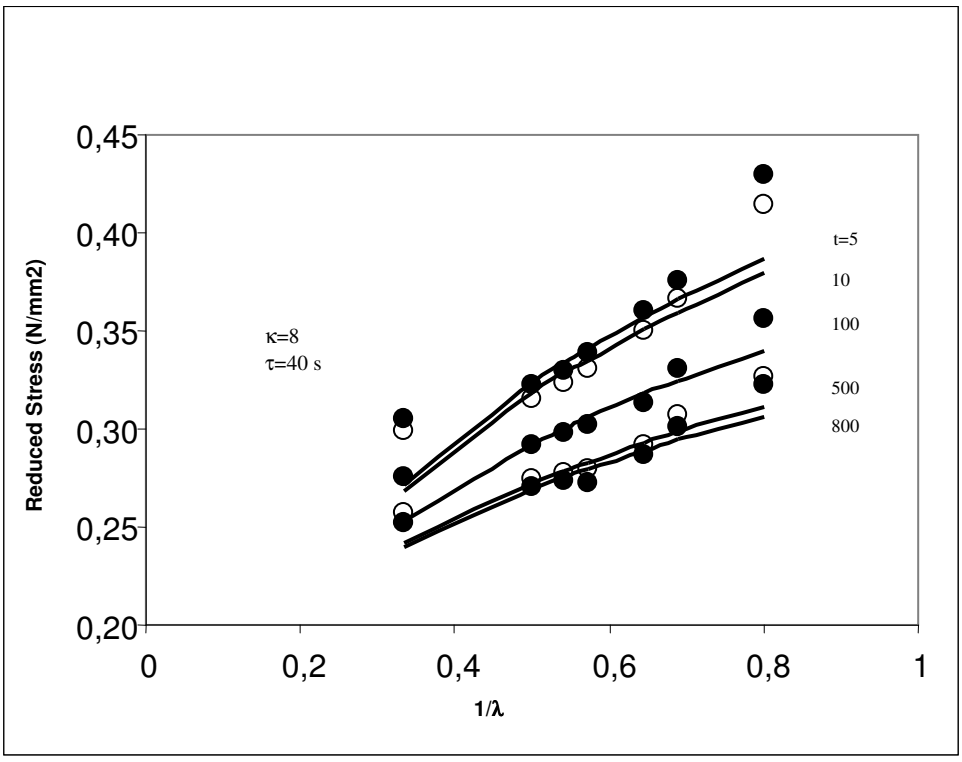

Figure 4.15 Isochronous plots of Sample S33 and comparison with the Dynamic Constrained Junction Model and results.

In Fig. 4.16-4.24 the dependence of stress on time is presented for all samples.

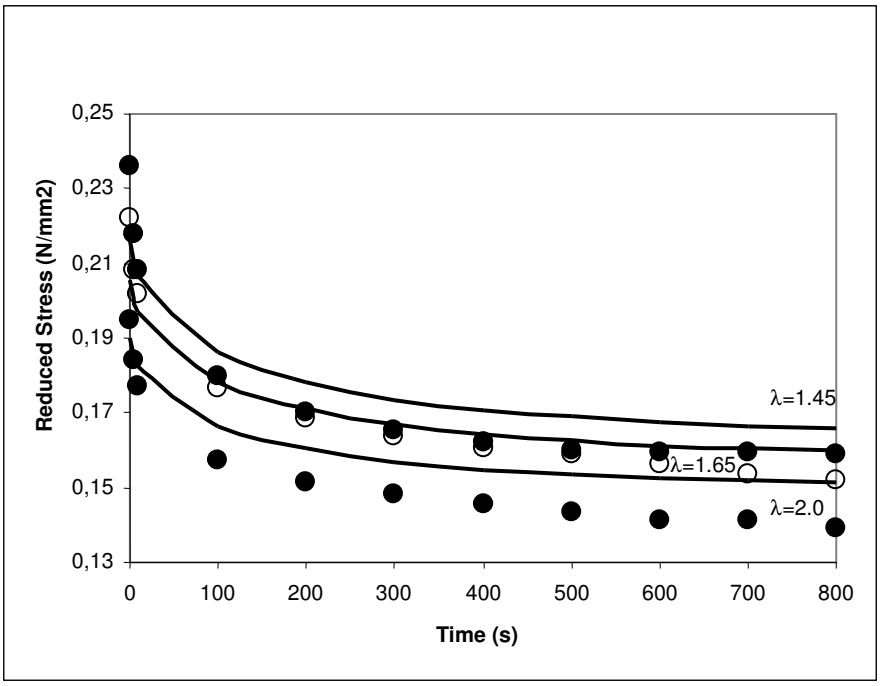

Figure 4.16 Dependence of stress on time for Sample 11

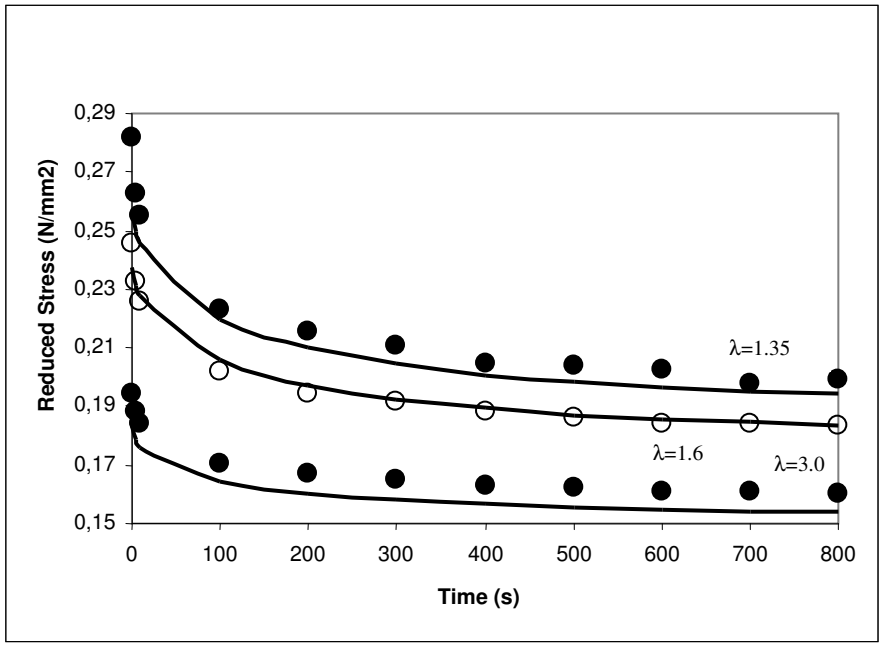

Figure 4.17 Dependence of stress on time for Sample 12

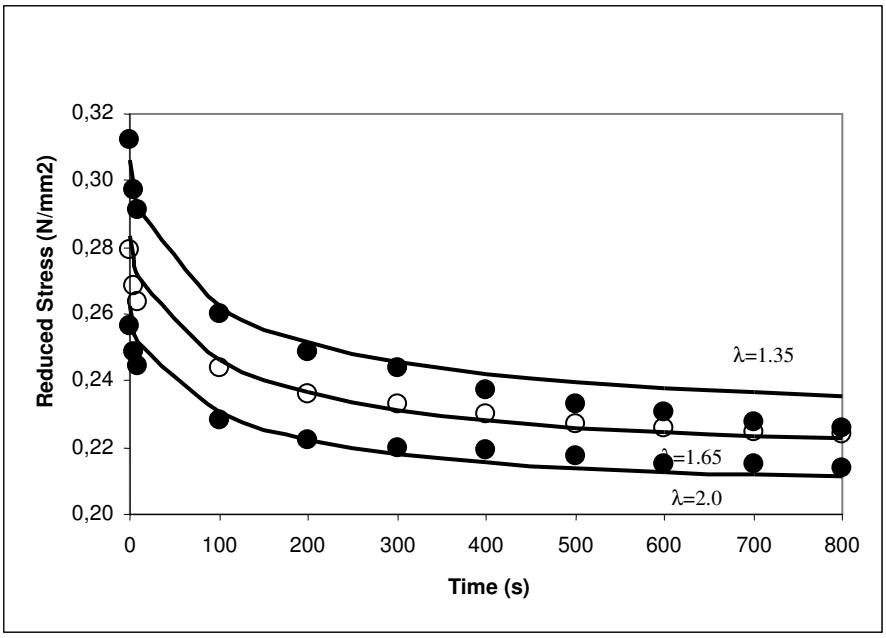

Figure 4.18 Dependence of stress on time for Sample 13

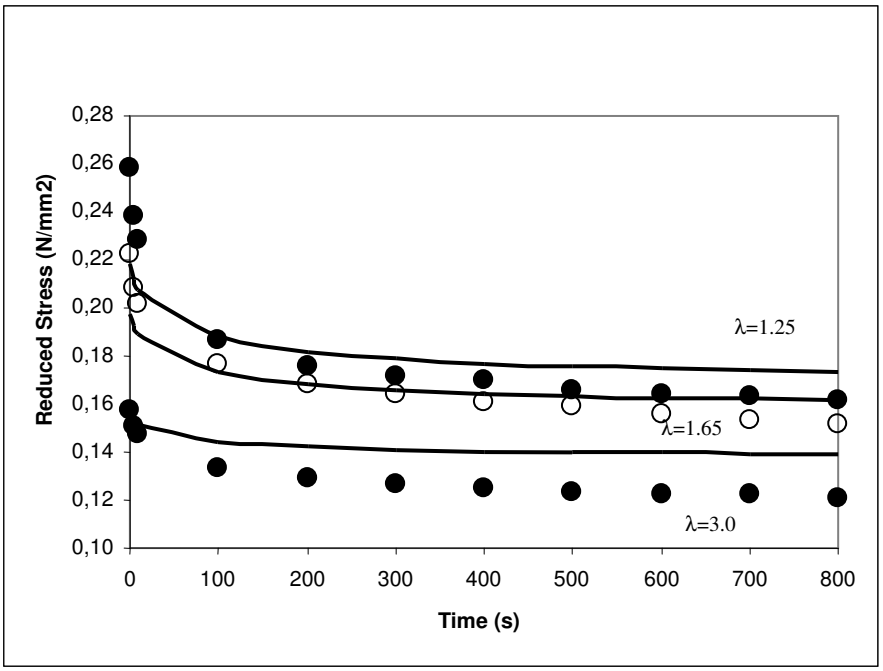

Figure 4.19 Dependence of stress on time for Sample 21

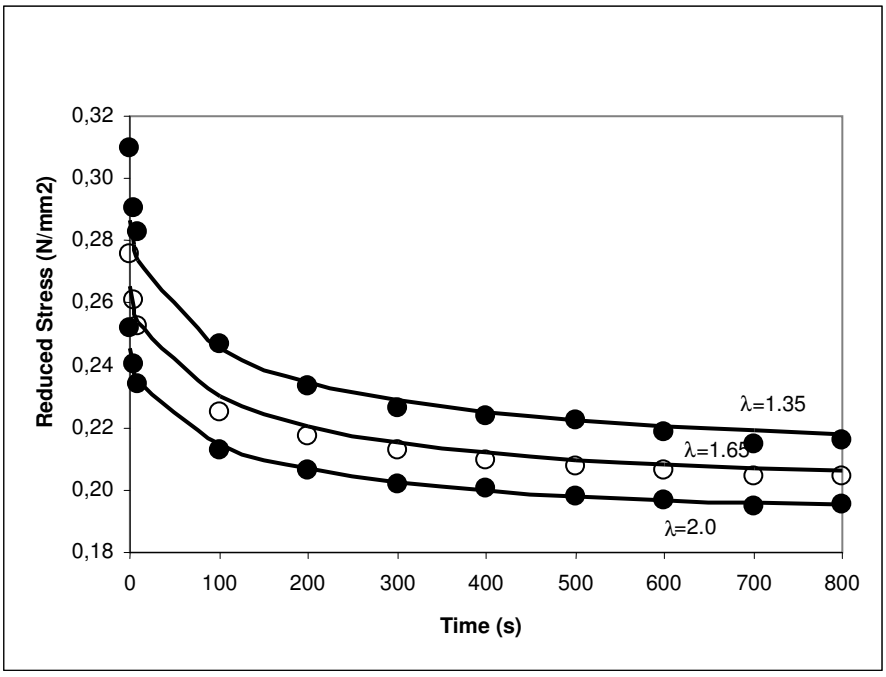

Figure 4.20 Dependence of stress on time for Sample 22

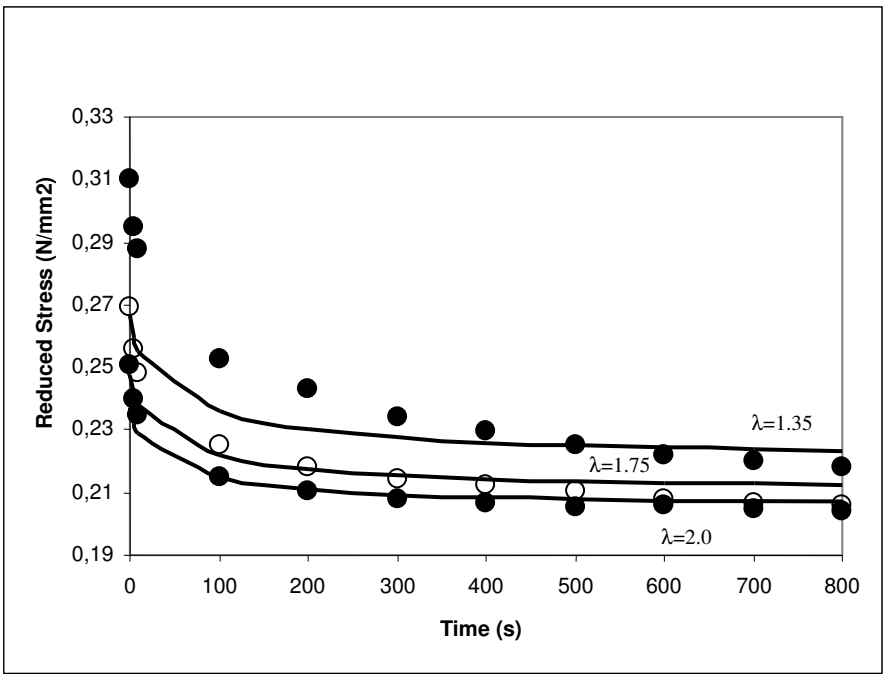

Figure 4.21 Dependence of stress on time for Sample 23

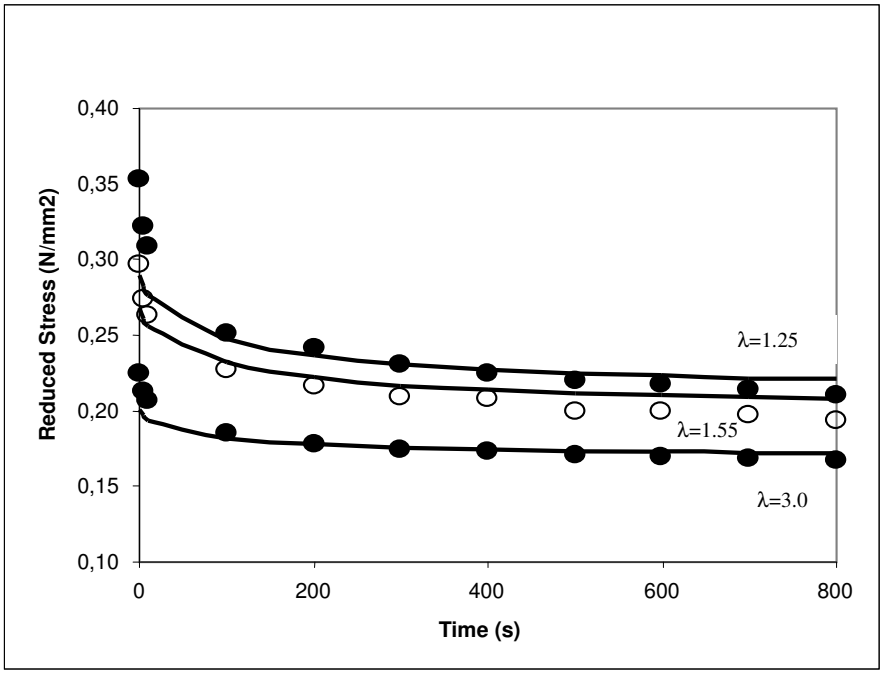

Figure 4.22 Dependence of stress on time for Sample 31

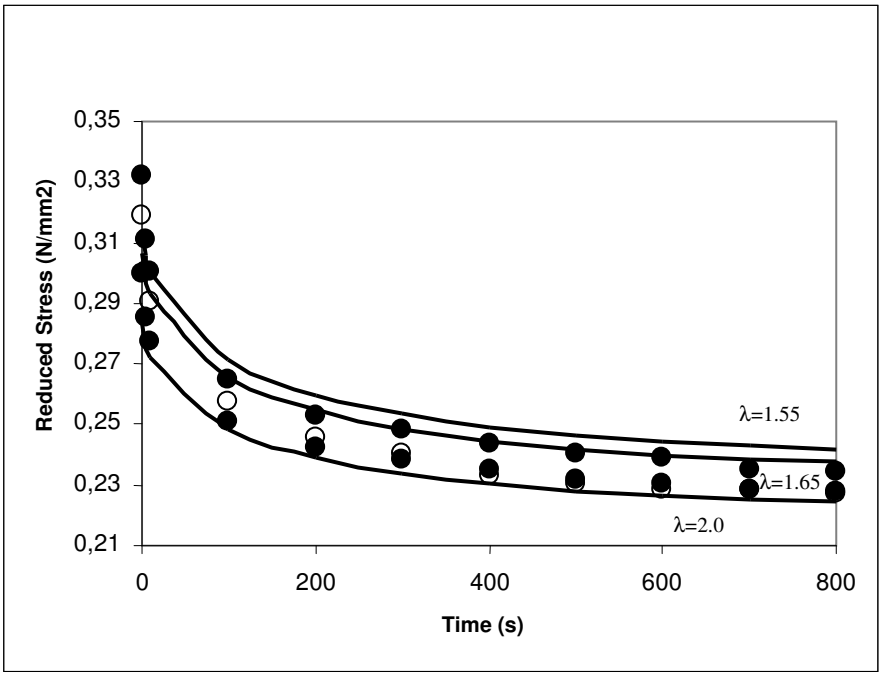

Figure 4.23 Dependence of stress on time for Sample 32

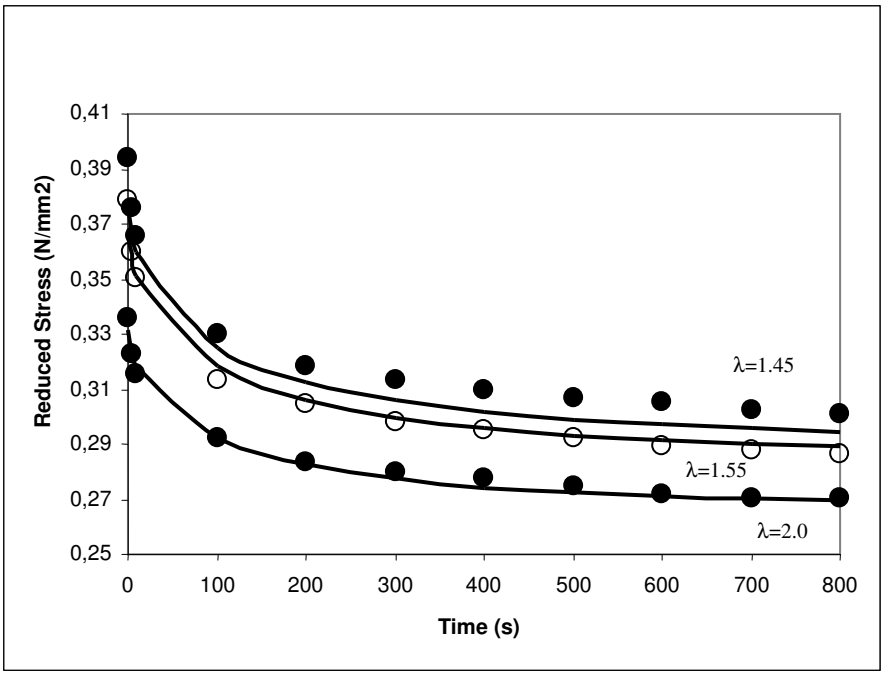

Figure 4.24 Dependence of stress on time for Sample 33

In this section, we extended the Dynamic Constrained Junction Model to stress relaxation of filled samples with different cross-link densities in uniaxial tension. The basic assumption that we made is the Guth and Gold equation dependence of the phantom, equilibrium and non-equilibrium forces acting on the network. We also used the occluded rubber for the effective volume of the fillers as proposed by Medalia. In Dynamic Constrained Junction Model there were 4 fitting parameters as given in unfilled section namely, phantom contribution (f_{ph}), relaxation time, τ, exponent, β and κ_0 . Since we used the same cross-link densities in the unfilled section, we used 3 parameters out of 4 as they were found in unfilled section. We only used κ_0 as the fitting parameter in the filled section. Results showed that the assumption that we have made for the filled elastomers really work well for capturing the stress relaxation behavior. Results revealed that the theory for the filled elastomers is well capturing the results irrespective of the filler amount. It means that this theory can be applicable for higher loadings as well. In some of the graphs there are some deviations from the experiment which are most probably due to the difficulty in nature of preparing the compounds and samples.

CHAPTER 5

5. CONCLUSION

One of the most important properties of the rubber is the viscoelastic property. Therefore, researches have been working on this subject for a long time. Generally, studies can be characterized based on two approaches: the kinetic theory which is based on the statistical thermodynamics considerations, and the phenomenological approach which treats the material as a continuum regardless of its micro-structural and molecular nature. One of the most important molecular based theories is the Constrained Junction Model. It has two contributions; one is from the phantom network and the other one is from the entanglements. Mooney Rivlin is the famous phenomenological approach to this subject.

In this study, Constrained Junction model is extended to the analysis of relaxation of amorphous networks. Experiments were carried out on natural rubber (NR) based compounds. Results can be subdivided into two categories. First category is for the unfilled samples and the second category is for the filled samples. For both categories, 3 different sulphur amounts (in other words, 3 different crosslink densities) were used. For the filled category, 3 different filler loadings were used.

Constrained Junction Model is used for networks at equilibrium. In this study, it is extended to the analysis of relaxation of the networks. It is made time dependent and named as Dynamic Constrained Junctions model. It is assumed that the κ parameter which is the measure of the strengths of the constraints in the model follow the stretched exponential form for the network relaxations. It is assumed that κ has the following form for the relaxation of the networks; $\kappa(t) = \kappa_0 \exp\left[-\left(\frac{t}{\tau}\right)^{\beta}\right]$. Experimental results showed that the isochronous Mooney plots can be well captured with the Dynamic Constrained Junction Model for three

different cross-link densities. This model also works well in predicting the dependence of stress on time for all cross-link densities studied. Therefore, for this unfilled category we can conclude that our new theory can be used for the relaxation of the unfilled amorphous networks.

In the second part of the study, filled elastomers were studied. In order to be able to adopt the Dynamic Constrained Junction Model for the filled elastomers, we made use of the Guth and Gold viscosity relation which is based originally on the Einstein's rule of viscosity for the suspended particles. Guth and Gold viscosity relation has the following form; $\eta^* = \eta(1 + 2.5\phi + 14.1\phi^2)$. The applicability of this relation to Young's modulus for filled polymers was studied by others. For this filled category our assumption is that this form can also be used for the phantom, equilibrium and non-equilibrium forces in the Dynamic Constrained Junction model. Therefore, phantom, equilibrium and non-equilibrium forces have the following form in Dynamic Constrained Junction Model, respectively; $f_{ph} = (f_{ph})_0 (1 + 2.5\phi + 14.1\phi^2)$, $f_{c,eq} = (f_{c,eq})_0 (1 + 2.5\phi + 14.1\phi^2)$, $f_c(t) = (f_c(t))_0 (1 + 2.5\phi + 14.1\phi^2)$. We also used that filler volume should be effective filler volume which takes into account the occluded rubber in the matrix. Experimental results showed that isochronous Mooney Plots and dependence of stress on time for filled elastomers can be captured with this new model as well. There are some deviations in some of the samples. These can be attributed to the difficulty of preparing the filled samples. A good dispersion and distribution of the fillers in the matrix was difficult for these samples.

In conclusion, we can say that this new theory, namely Dynamic Constrained Junction Model, can well capture the relaxation of amorphous networks in unfilled and filled state. It has the advantage over other theories in that the Dynamic Constrained Junction model has a very good molecular basis since it is the adoption of Constrained Junction Model to the relaxation of amorphous networks.

For future work, we can say that this new theory can be examined for different deformation modes such as compression, or shear, or multiaxial loading.

6. REFERENCES

1. Strong, A.B., *Plastics Materials and Processing*, Prentice Hall, New Jersey, 1996

2. Billmeyer, F.W.,*Textbook of Polymer Science*, John Wiley Sons., New York, 1984

3. Flory, P.J., *Principles of Polymer Chemistry*, Cornell University Press, London, 1953

4. Treloar L.R.G., *The Physics of Rubber Elasticity*, Clarendon Press, Oxford, 1975

5. Brydson, J.A., *Rubbery Materials*, Elsevier Applied Science, London, 1988

6. F.L. Abbes, P.Ienny, R.Piques, *Polymer*, 44, 821, 2003

7. J.E.mark, B.Erman, F.R.Eirich, "*Science and Technology of Rubber*", Academic Press, London, 1994

8. J.E.Mark, B.Erman, "*Rubberlike Elasticity, A molecular Primer*", Wiley, London, 1988

9. Erman B., Mark J.E., *Structure and Properties of Rubberlike Networks*, Oxford University Press, New York, 1997

10. Flory, P.J., *British Polymer Journal*, 17, 96, 1985

11. Flory, P.J., *Polymer*, 20, 1317, 1979

12. Flory, P.J. *J. Chem. Phys.*, 66, 5720, 1977

13. M. Rubinstein, R.H.Colby, "*Polymer Physics*", Oxford University Press, New York, 2003

14. J.W.M. Noordermeer, J.D. Ferry, *J.Polym. Sci. Polym. Physc.* Ed., 14, 509, 1976

15. B.Erman, W.Wagner, P.J.Flory, *Macromolecules*, 13,1554, 1980

16. W.W. Graessley, *Polymeric Liquids and Networks, Structure and Properties*, New York, Taylor and Francis, 2007

17. N.R. Langley, K.E. Polmanteer, *J. Polym. Sci. Polym. Phys. Ed.*, 12, 1023, 1974

18. N.Rennar, W.Oppermann, *Colloid. Polym. Sci.*, 270, 527, 1992

19. R.J.Spontak, R.L. Roberge, M.S. Vratsanos, W.E. Starner, *Polymer*, 41, 6341, 2000

20. E.Ehabe, F.Bonfils, C.Aymard, A.K. Akinlabi, J.S.Beuve, *Poly.Testing*, 24, 620, 2005

21. S.A. Baeurle, A.Hotta, A.A.Gusev, *Polymer*, 46, 4344, 2005

22. C.Ortiz, C.K.Ober, E.J.Kramer, *Polymer*, 39, 3713, 1998

23. S. Ronan, T.Alshuth, S.Jerrams, N.Murphy, *Mat.&Desig*, 28, 1513, 2007

24. A.D.Drozdov, A.Dorfmann, *Int. J.Sol.and Struc*., 39, 5699, 2002

25. A.Hotta, S.M.Clarke, E.M.Terentjev, *Macromolecules*, 35, 271, 2002

26. S.Toki, T.Fujimaki, M.Okuyama, *Polymer*, 41, 5423, 2000

27. M.Tosaka, Y.Ikeda, S.Toki, B.S.Hsiao, *Macromolecules*, 39, 5100, 2006

28. V.P. Privalko, S.M.Ponomarenko, E.G. Privalko, F.Schön, W.Gronski, E.*Polym.J*., 41, 3042, 2005

29. A.Batra, C.Cohen, L.Archer, *Macromolecules*, 38, 7174, 2005

30. V.G. Geethamma, L.A.Pothen, B.Rhao,N.R.Neelakantan, S.Thomas, *J.Appl. Polym. Sci*., 94, 96, 2004

31. A.R.R.Menon, *J.Appl.Polym.Sci*., 65, 2183, 1997

32. L.Zanzotto, J.Stastna, *J.Polym.Sci B:Polym Phys*, 35, 1225, 1997

33. T.M.Madkour, *J. Appl. Polym. Sci*, 92, 3387, 2004

34. H.M.Osman, S.A.A.Ghani, T.M.Madkour, A.R.Mohamed, *J.Appl.Polym.Sci*., 77, 1067 2000

35. G.R.Cotten, B.B.Boonstra, *J.Appl.Polym.Sci*., 9, 3395, 1965

36. S.Franklin, C.Chang, *J.Appl.Polym.Sci*., 8, 37, 1964

37. L.T.Smith, *J.Polym.Sci. Partc:Polym. Symp*., 16, 841, 1965

38. C.I. MacKenzie, J.Scanlan , *Polymer*, 25, 559, 1984

39. G.M. Bartenev, N.M. Lyalina, *Polymer Science. Series A*, 12, 1049, 1970

40. E.Guth, O.Gold *Physical Review*, 53, 322, 1938

41. E.Guth, *J.Appl. Physc*, 16, 20, 1945

42. H.M. Smallwood, *J.Appl. Physc*, 15, 758, 1944

43. A.I. Medalia, *Rubber Chemistry and Technology*, 45, 1171, 1972

44. K.L. Ngai, C.M. Roland, *Macromolecules*, 27, 2454, 1994

45. B.Erman, P.J.Flory, *Macromolecules*, 15, 806, 1982

46. B.Ewen, D.Richter, In: J.E. Mark, B.Erman, editors. *Elastomeric Polymer Networks,* Prentice Hall, Englewood Cliffs, p.220-234, 1992

47. H.B. Callen, *Thermodynamics and an introduction to thermostatistics*, Wiley, New York, 1985

48. R.Chasset, P.Thirion., *Proceedings of the conference on physics of non- crystalline solids*, 264, 345, 1965

49. R.G. Palmer, D.L. Stein, E. Abrahams, P.W.Anderson, *Phys. Rev. Let*., 53, 958, 1984